AD-A032 375 NAVAL POSTGRADUATE SCHOOL MONTEREY CALIF F/G 1/3
MAN-POWERED FLIGHT.(U)
SEP 76 L CARTER

UNCLASSIFIED NL

1 OF 1
AD A032375

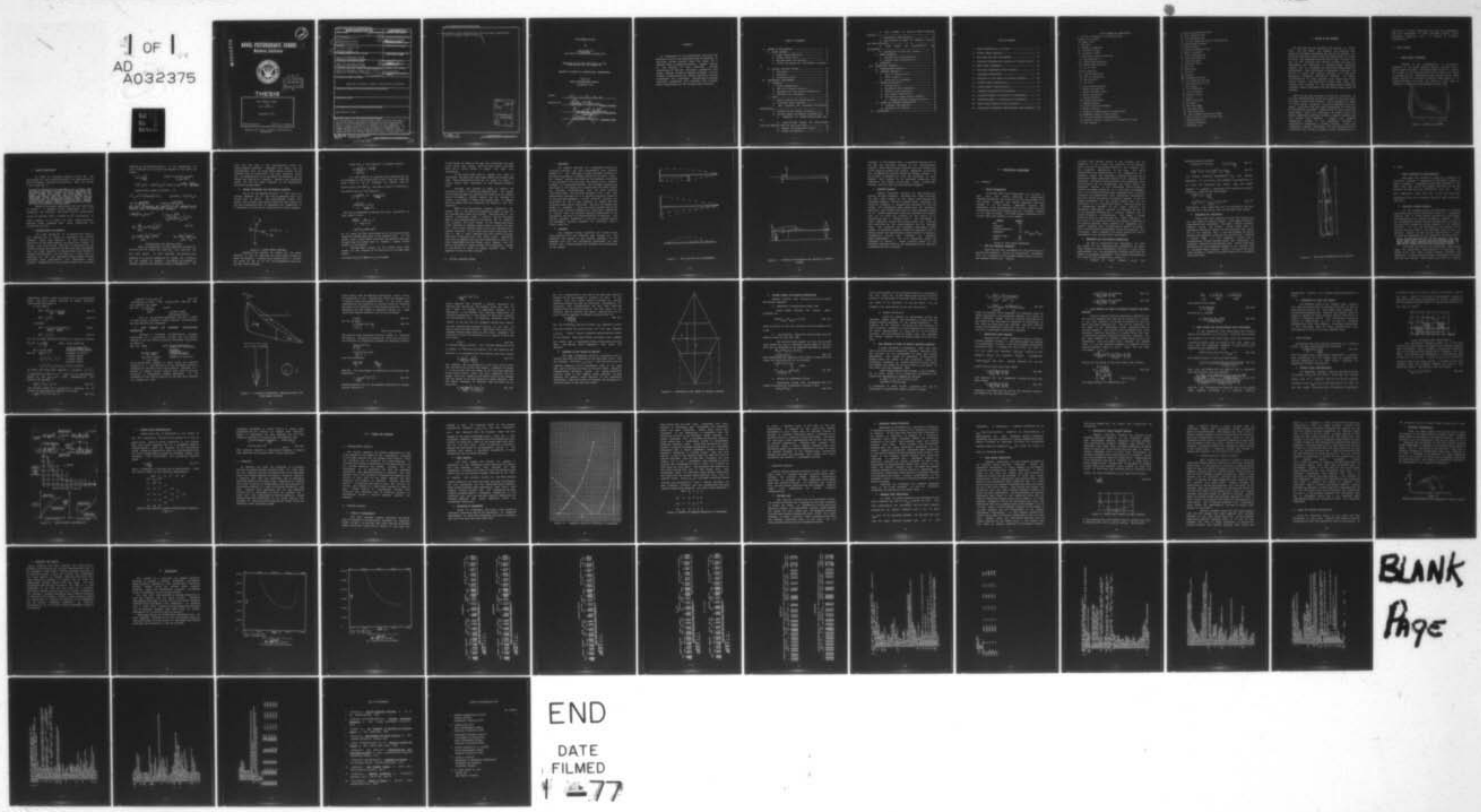

BLANK Page

END

DATE FILMED
1-77

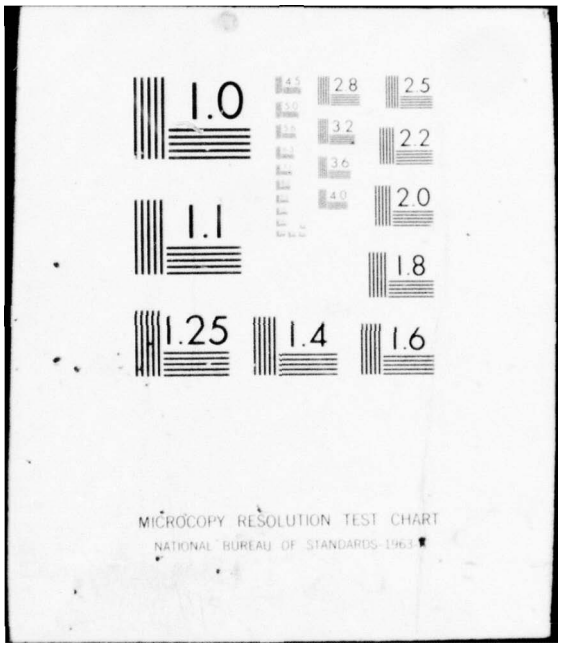
1.0
1.1
1.25
1.4
1.6
1.8
2.0
2.2
2.5
2.8
3.2
3.6
4.0
MICROCOPY RESOLUTION TEST CHART
NATIONAL BUREAU OF STANDARDS-1963-A

(2)

NAVAL POSTGRADUATE SCHOOL
Monterey, California

THESIS

MAN-POWERED FLIGHT

by

Lynn Carter II

September 1976

Thesis Advisor: Milton U. Clauser

SECURITY CLASSIFICATION OF THIS PAGE (When Data Entered)

REPORT DOCUMENTATION PAGE

READ INSTRUCTIONS BEFORE COMPLETING FORM

1. REPORT NUMBER

2. GOVT ACCESSION NO.

3. RECIPIENT'S CATALOG NUMBER

4. TITLE (and Subtitle)

(6) MAN-POWERED FLIGHT,

(9) 5. TYPE OF REPORT & PERIOD COVERED

MASTER's Thesis; (September 1976)

6. PERFORMING ORG. REPORT NUMBER

7. AUTHOR(s)

(10) Lynn Carter, II

8. CONTRACT OR GRANT NUMBER(s)

9. PERFORMING ORGANIZATION NAME AND ADDRESS

Naval Postgraduate School
Monterey, California 93940

10. PROGRAM ELEMENT, PROJECT, TASK AREA & WORK UNIT NUMBERS

11. CONTROLLING OFFICE NAME AND ADDRESS

Naval Postgraduate School
Monterey, California 93940

(11) 12. REPORT DATE

September 1976

13. NUMBER OF PAGES

14. MONITORING AGENCY NAME & ADDRESS (if different from Controlling Office)

Naval Postgraduate School
Monterey, California 93940

(12) 53 p.

15. SECURITY CLASS. (of this report)

Unclassified

15a. DECLASSIFICATION/DOWNGRADING SCHEDULE

16. DISTRIBUTION STATEMENT (of this Report)

Approved for public release; distribution unlimited.

17. DISTRIBUTION STATEMENT (of the abstract entered in Block 20, if different from Report)

18. SUPPLEMENTARY NOTES

19. KEY WORDS (Continue on reverse side if necessary and identify by block number)

Man-Powered Flight

20. ABSTRACT (Continue on reverse side if necessary and identify by block number)

An alternative to the conventional rigid wing was explored to see if any advantage might be obtained by utilizing slotted airfoil sails for wings and a complete shift in emphasis towards a lighter vehicle at the expense of drag penalties. Optimum combinations of size and structural parameters were sought through extensive computer analysis. Various tradeoff considerations for further improving aircraft structural → next page

DD FORM 1 JAN 73 1473 (Page 1)

EDITION OF 1 NOV 65 IS OBSOLETE
S/N 0102-014-6601

SECURITY CLASSIFICATION OF THIS PAGE (When Data Entered)

251450

4B

parameters were obtained with aircraft power requirements and the optimum flight velocity.

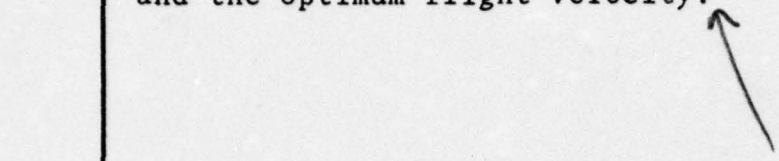

MAN-POWERED FLIGHT

by

Lynn Carter II
Lieutenant
B.S. United States Naval Academy, 1968

Submitted in partial fulfillment of the
requirements for the degree of

MASTER OF SCIENCE IN AERONAUTICAL ENGINEERING

from the
NAVAL POSTGRADUATE SCHOOL
September 1976

Author: Lynn Carter II

Approved by: Melton H Clausen
Thesis Advisor

Daniel J. Collins
Chairman, Department of Aeronautics

J R Borsting
Academic Dean

ABSTRACT

An alternative to the conventional rigid wing was explored to see if any advantage might be obtained by utilizing slotted airfoil sails for wings and a complete shift in emphasis towards a lighter vehicle at the expense of drag penalties. Optimum combinations of size and structural parameters were sought through extensive computer analysis. Various tradeoff considerations for further improving aircraft performance were considered. Predictions of optimum structural parameters were obtained with aircraft power requirements and the optimum flight velocity.

TABLE OF CONTENTS

LIST OF FIGURES

LIST OF SYMBOLS AND ABBREVIATIONS

A constant of integration, collection of terms

α angle of inclination

AR aspect ratio

b wing span

B constant of integration

B_i collection of terms

B_o collection of terms

c wing chord, column end conditions

C_d drag coefficient

C_{di} induced drag coefficient

C_{do} parasite drag coefficient

c_j jib sail chord

C_l lift coefficient

C_{lw} wing lift coefficient

C_{lt} tail lift coefficient

c_m main sail chord

c_o root chord

c_p parasite drag coefficient

d midspan sail deflection

e Oswald's efficiency factor

E modulus of elasticity

f parasite drag area

GW aircraft gross weight

h spreader distance

h/b height above ground/wingspan

I moment of inertia

K reduction of induced drag due to ground effect

K_d deflection constant of proportionality

K_t tail area constant of proportionality

L_w distance from center of gravity to lifting force of wing

P power, pressure

P_g power including ground effects

P_i inner compressive load

P_o outer compressive load

P_{cr} critical compressive load for column buckling

P_n interpolating polynomial

q dynamic pressure

Q inverse of slenderness ratio

R radius of curvature

R_1 outer restraining stay

R_2 inner restraining stay

r_o outer spar radius

r_i inner spar radius

S sail area

SF safety factor

S_t tail area

S_w wing area

σ_θ circumferential stress

σ_s sail weight per unit area

T tension from force of sail

t spar thickness

TL tail lifting force

T_j jib sail tension

T_m main sail tension

v velocity

W weight of aircraft

W_b body weight

W_i inner spar weight

W_o outer spar weight

WL wing lifting force

WL' wing lifting force minus sail weight

X ratio of outer to inner wing spar radii

y distance along spar

z deflection above span

Z slenderness ratio

I. NATURE OF THE PROBLEM

For centuries man has dreamed of the freedom of flight under his own power. The prospect has received much attention and effort throughout the history of mankind. Yet since the time that Icarus spread his wings above the shores of Crete, such endeavors have had little more success than that of the Athenian. This century, however, has seen the development and refinement of lighter, stiffer materials coupled with an increased and quantified understanding of aerodynamics. This combination of increased awareness and ability to solve the problem resulted in a string of marginally successful man-powered aircraft. One common characteristic of these machines was a rigid wing of one form or another. The possibility exists that other wing designs more suitable to the low-speed-flight regime and stringent weight requirements of man-powered flight might be feasible.

While man has been dreaming of flight for centuries, he has been simultaneously plying the oceans of the world under the power of sail-driven vessels. Sails provided the means to drive ships, generally in winds of moderate force and speed. Sails have also been used successfully for centuries on high-powered windmills. Modern sails are both strong and quite light. Could the technology of modern sails and modern lightweight materials provide a lighter flexible wing than current rigid designs? A jibsail and mainsail combination rotated to the horizontal provides a configuration resembling a slotted airfoil. Could this combination produce sufficient lift and tolerable drag at acceptable power levels to produce a viable alternative to a

rigid wing? Is there a difference in rigid wing performance and sail performance in this low-speed regime? These intriguing questions were the subject of extensive consideration.

A. HUMAN ELEMENT

1. Power Versus Endurance

Foremost in the consideration of man-powered aircraft is the human being's ability to supply only a finite amount of power. This power must be used to support the weight of the pilot and his craft as well as to propel it through the air. References 6 and 8 showed man's power output ability as a function of exertion time (Figure 1). It clearly dictates the power for which a craft must be designed to operate for any specified flight time.

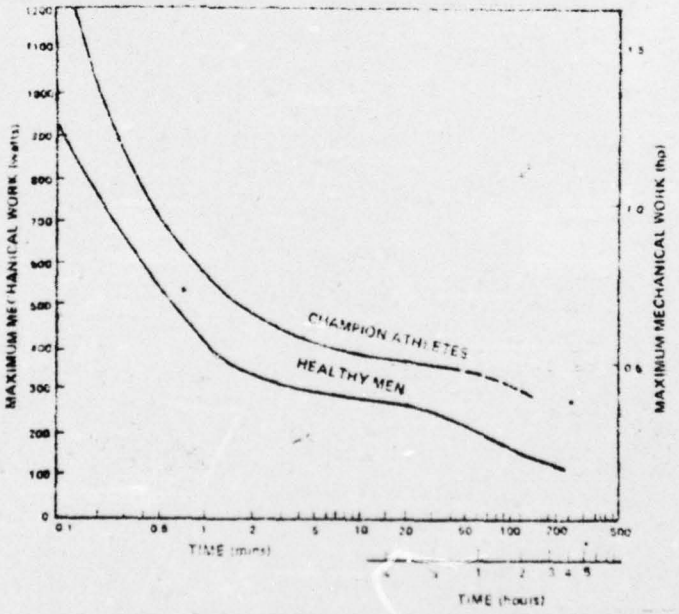

Figure 1 -POWER VS• LOG TIME

2. Kremer Competition

In order to establish specific goals for the performance of a man- powered aircraft, the requirements set forth by Kremer, a British industrialist. They are quoted in part from Ref. 8.

> A prize of L10,000 will be awarded to an entrant from any part of the world who first fulfills the conditions. The course shall be a figure of eight embracing two turning points which shall not be less than 1/2 mile apart. It must be ensured that the machine is in continuous flight over the entire course and must be flown clear of and outside each turning point. Ground clearance will be minimum of 10 feet at start and also at the finish, both to which are the same point halfway between the turning points. Between start and finish the ground clearance is unrestricted.

Based on the Kremer requirements and the limitations of Figure 1 a designed flight requirement of .3-.4 horsepower was selected. The craft had to be maneuverable enough to negotiate turns in excess of 180^{o} and operate, at least briefly, at or above ten feet ground clearance. Aircraft design proceeded with these objectives and limitations in mind.

3. Optimum Power and Velocity

The first derivative of an equation set equal to zero enables one to obtain an expression for certain optimums within that equation. In this instance the derivative of the power equation was taken with respect to velocity and set to zero. From this an expression for the optimum velocity was obtained and when this was reintroduced into the power equation an optimum power with respect to velocity was obtained. This was done as a first step in searching for the most desireable flight regime and best obtainable power requirements. The development below develops expressions for the optimum velocity and the power

required at the optimum velocity. In the development the lift developed by an aircraft was assumed to just equal its weight.

$$C_d = C_{do} + \frac{Cl^2}{\pi ARe}$$

P=power to propel aircraft

$$W = \tfrac{1}{2}\rho V^2 C_L S$$

$$P=\rho v^2 C_d Sv/2 = .5\rho Sv^3[C_{do}+Cl^2/ARe] = \tfrac{1}{2}\rho S V^3 C_{D_o} + \frac{2W^2}{\rho V S \pi e}$$

minimum power occurs at dP/dv=0 or:

$$3v^2 C_{do} = W^2 v^2/[S\pi ARe(\rho v^2/2)^2] \qquad \text{therefore: } P=\rho v^3 S4C_{do}/2$$

$$.5\rho v^2 = W/S\sqrt{3C_{do}\pi ARe} \qquad P=4SvC_{do}W/S\sqrt{3C_{do}\pi ARe}$$

The first derivative was solved and an expression for velocity was substituted back into the original power equation which was subsequently regrouped.

$$v=\sqrt{2W/\rho S}/(3C_{do}\pi ARe)^{.25} \qquad P=\frac{4C_{do}W}{3C_{do}\pi ARe}\sqrt{\frac{2W}{\rho S}}\frac{1}{(3C_{do}ARe)^{.25}}$$

$$P_{opt.}=\frac{4\sqrt{2}}{(3\pi e)^{.75}}\frac{C_{do}^{.25}W^{.25}}{AR^{.75}} \qquad AR=b^2/S$$

$$P_{opt.}=\frac{4(2/\rho)^{.5}(f)^{.25}(W/b)^{1.5}}{(3\pi e)^{.75}} \qquad V_{opt}=\frac{(2/\rho)^{.5}(W/b)^{.5}}{(3\pi e)^{.25}(f)^{.25}}$$

optimum power and velocity terms

Terms of significance in both equations included the parasite area "f" (where f=S times Cd_o) and wing-lift per unit span (WL/b). In both equations the parasite area appeared to be fairly insensitive to change and therefore not the subject of concern. Its effect was examined in computer analysis and receives attention subsequently. The

term WL/b was seen to more significantly affect the power-required equation. Therefore the search for the configuration with the least power became a search for the airplane with the lowest WL/b. The most desirable locale for the demonstration is at sea-level and therefore the air density was treated as a constant. Oswald's wing efficiency factor (e) was the final variable to be examined for obtaining optimum power.

4. Glider Philosophy and Man-Powered Aircraft

All of the man-powered aircraft to date have put obvious emphasis on low drag and streamlining even at an obvious cost in weight. Any knowledgeable reader will wonder who is wrong, particularly when the best gliders are the fast streamlined ones. To understand the comparison it is necessary to first better understand the glider problem:

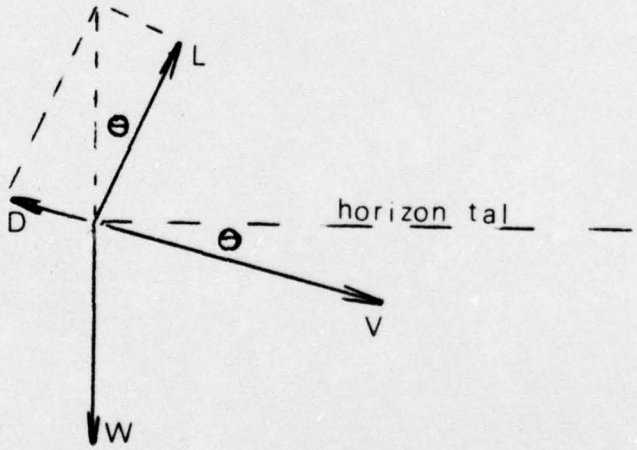

Figure 2. GLIDER VECTOR ANALYSIS

Because of the balance of forces and the above geometry it can be seen that the glide slope or angle is equal to Drag/Lift. A glider pilot simply wants to stretch his glide as far as he can and consequently wants the flattest angle possible.

Tying this to the algebraic in simplest concept:

$$\frac{D}{L}=\frac{.5\rho v^2\left[C_d+C_1^2/\pi AR\right]S}{.5\rho v^2 C_1 S}$$

In this equation Cd (parasite drag coefficient) may be considered to be constant but Cl and V both vary when the pilot tries to fly at different air speeds. They are related since $L=W=.5\rho v^2 C_1 S$ and this is used to eliminate C_1 and retain only V in the equation.

$$\frac{D}{L}=\frac{.5\rho v^2 S\left(Cd_o+\left(W/.5 v^2 S\right)^2\right)}{W}$$

$$=\frac{.5\rho v^2 SCd_o}{W}+\frac{W}{\pi AR.5 v^2 S}$$

This can be minimized by setting the first derivative of (D/L) equal to zero

$$\frac{\rho vSCd_o}{W}-\frac{2W}{\pi AR.5 v^3 S}=0$$

$$.5\rho v^2 SCd_o=W/\pi AR.5\rho v^2 S$$

Or in words, the best glide angle is at the velocity which makes the induced drag equal to the parasite drag. If the glider pilot flies faster than this the parasite drag goes up more than the induced drag is reduced. Slower flight results in the reverse.

Interestingly enough, if the glider pilot adds weight to his airplane he can still fly at the same glide angle:

$$D/L=Cd/Cl=(Cd_o+Cl^2/\pi AR)/Cl=Cd_o/Cl+Cl/\pi AR$$

If the glider is flown at the same lift coefficient the same glide angle will result. With the extra weight the craft will fly a little faster to regain the same lift coefficient.

If the glider pilot were to improve his craft by increasing the span then that would reduce the induced drag term. Extra advantage of this can be taken by flying a little slower than previously to also decrease parasite drag.

Fairings may instead be added to improve the airplane in order to reduce the parasite drag. The weight of the fairings does not penalize the glider but the reduced drag is of benefit. Further benefit can be obtained by flying a bit faster to reduce the induced drag. In summary drag and aspect ratio are important but weight is not very important.

Where is the man-powered airplane different? The energy that a man puts into sustaining flight is equal to the airplane drag times the velocity. Relating this to the glider: power=(D/L) times V times W. The D/L indicates some of the characteristics of the glider but in addition must consider the W and V terms. In the glider, additional weight resulted in slightly faster flight to regain the same D/L , but in this instance both W and V will increase for a similar situation. On the other hand weight reductions mean both W and V would decrease even with reduced velocity sufficient to maintain the s ame glide angle. Apparently this kind or argument has not been recognized by some of the other competitors for the Kremer prize because they all seem to be trying to design gliders with propellers. Weight is sacrificed in order to reduce parasite drag. The opposite is true of this analysis.

B. INITIAL AIRCRAFT DESIGN

1. Sail-Wing

For reasons detailed in a subsequent section the following wing-spar and sail arrangements were selected (Figure 2). The semi-span of each wing-spar consisted of two hollow cylinders of unequal radius but of equal length. The inboard cylinder was fixed at the fuselage, stabilized at its extremity by a wire stay, and joined to the outboard cylinder in a pin-ended fashion. The outboard cylinder was restrained at the wingtip by a second wire stay which joined the fuselage coincidentally with the inner fuselage restraining wire. Two vertical spreaders with stays were positioned at mid-span so as to provide structural integrity to the wing-spar segments. A third vertical spreader was positioned on top of the fuselage to support the wing structure under static conditions. The sail arrangement was chosen to resemble a genoa jib which overlaps 50% of the mainsail and a mainsail combination. When this combination is rotated from the vertical (sailing orientation) to the horizontal, one wing of a slotted airfoil is obtained. The initial analysis considered a wing with a pointed wingtip and subsequent analysis examined the trade-offs with a finite chord tip.

2. Fuselage

The fuselage design consisted of a single hollow tube referred to as the fuselage spar (Figure 4). The propeller was placed at the forward extremity of the fuselage with the man arbitrarily positioned two feet further aft. Shortly behind the propeller the leading edge of the jibsail

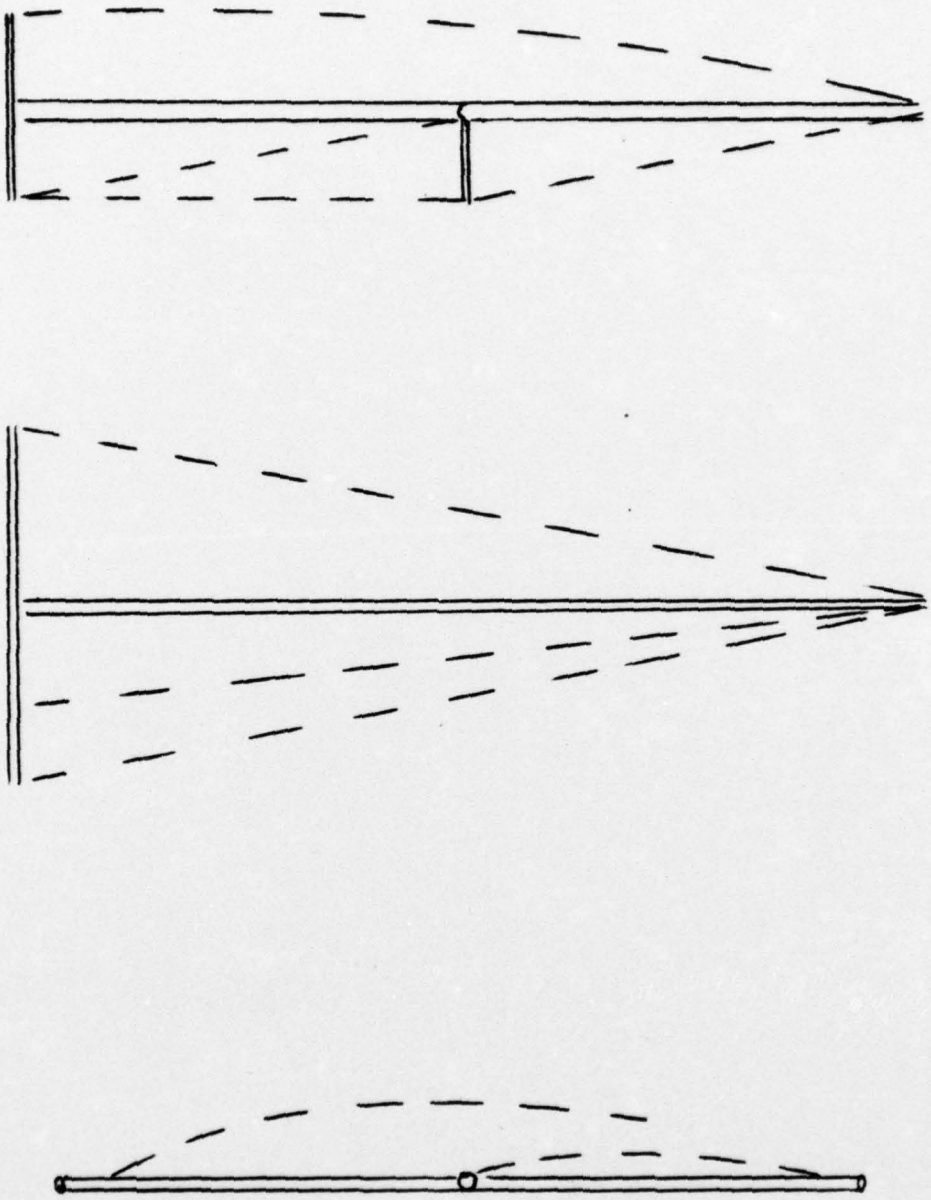

Figure 3 - WING SPAR AND SAIL ARRANGEMENT

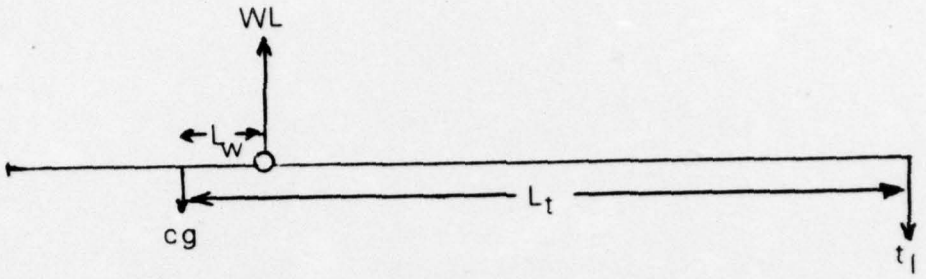

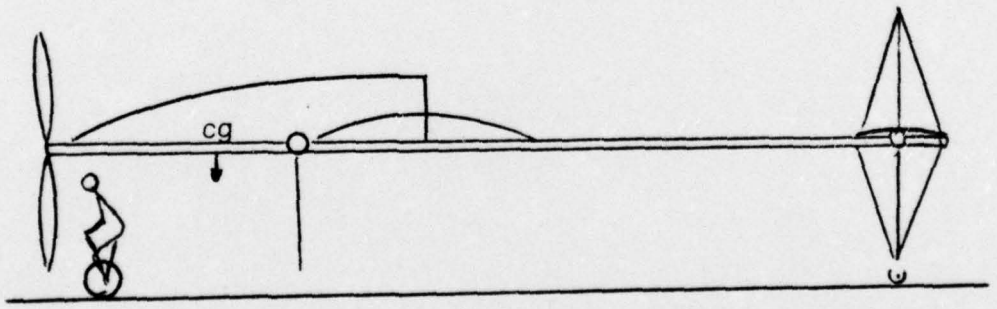

Figure 4 - FUSELAGE CONFIGURATION AND BALANCE OF LIFTING FORCES

attached to the fuselage spar. A specified distance aft of the man the wing-spar attached to the fuselage-spar. Directly above the wing-spar junction with the fuselage the static support spreader was located. Empennage positioning was determined by aircraft weight and balance criteria. To be as light as possible the size and thickness of these members were obliged to be optimized consistent with structural and safety limitations. These limitations, however, were not the only constraining elements.

3. Limiting Factors

Primary structural criteria for spar design were bending and Euler buckling. Therefore for a given strength, the spar grew lighter as the radiis was increased and thickness reduced. However to prevent local crippling and practical handling, a minimum wall thickness of .030" was chosen. Lift coefficient upper limits were not definitely specified, but attempts were made to avoid exceeding values of 1.5. Modern hang-glider wings have achieved Cl's greater than 2.0 in tests and Cl-stall in the region of 1.6 according to Ref. 9. Therefore Cl=1.5 was determined to leave sufficient margin for control, gusts, etc. Last and most important, was the power-required for the designed craft. The intention was to produce a prototype at least capable of traversing Kremer's course and preferably able to sustain flight for approximately twenty minutes in duration. Consequently efforts were directed at achieving power-requirements in the .3-.4 horsepower region as suggested by Figure 1. These criteria served as the principal limiting values in the minimizations and trade-off considerations that followed.

II. THEORETICAL DEVELOPMENT

A. FUSELAGE

1. Weight Assumptions

In the hope that this design might be utilized by more than the narrow spectrum of light-weight "champion-athletes", the weight of the man was assumed to be 180 pounds. Propeller and bicycle apparatus were each assumed to be ten pounds. Empennage weights were considered to be approximately 20% of their respective wing counterparts while the fuselage spar was initially assumed to be about 24 pounds. The "body weight" breakdown for an initial guess was selected at 240 pounds:

object	weight	
man	180	
propeller	10	
bicycle apparatus	10	
empennage	16	$.2(wt_{spars} + wt_{sail})$
fuselage spar	24	
TOTAL	240	

Figure 5. BODY WEIGHT BREAKDOWN

2. Man and Propeller Location

Three options were considered for the positioning of the man and propeller. First, the conventional arrangement with the propeller at the extreme forward position and the man somewhat further aft. Second,

the man in the forward region of the aircraft but the propeller at the extreme aft position of the fuselage. Third, the man in the forward region of the fuselage with the propeller immediately to his rear. The second configuration was abandoned due to the complexities of a propeller amidst the empennage structure and also due to anticipated weight penalties related to the extended drive mechanism. Although attractive from a drag standpoint (i.e. pilot forward of the slipstream) the third option was discarded because of the pronounced center-of-gravity effects and weight penalties of a man-first arrangement. Also, the structural difficulties associated with a rotating propeller on a bending beam were considered undesireable. The first option was chosen for several reasons. At the low speeds anticipated for the flight regime drag was not considered to be a significant factor. This was borne out in mathematical analysis of the power equation and subsequent experimental results. In addition, the man aft of the propeller provided for a shorter fuselage due to center-of-gravity considerations. This meant a weight reduction which in turn resulted in a power reduction. A man close to the center-of-gravity also meant a reduction in the bending stresses which enabled the employment of a lighter fuselage spar (thinner and/or smaller in radius). While unconventional arrangements of man and propeller were intriguing, there appeared to be valid reasons for what is considered as the "conventional" arrangement.

3. Empennage and Tail-Length Assumptions

For ease of calculations and flexibility the size and weight of the empennage were considered to be 20% of their respective wing counterparts. This was a good first approximation for the optimization analysis which kept the number of parameters manageable. Tail length considerations were based on the illustration in Figure 4.

A balance of force moments about the

center-of-gravity yielded:

$$Cl_w qS_w (L_w) = Cl_t qS_t (L_t) \qquad Cl_t S_t = Cl_w S_w \frac{L_w}{L_t} \qquad \text{Eqn (1)}$$

$$W = \frac{1}{2}\rho v^2 (Cl_w S_w - Cl_t S_t) = \frac{1}{2}\rho v^2 Cl_w S_w \left(1 - \frac{L_w}{L_t}\right) \qquad \text{Eqn (2)}$$

For reasons described subsequently "L_w" was assumed equivalent to $c_o/6$ and "L_t" was assumed to be equivalent to 1.5 times the wing-sail root chord. This was deemed adequate to provide a sufficient tail volume for aircraft stability. Equation (2) then became:

$$W = \frac{1}{2}\rho v^2 S_w Cl_w \left(1 - \frac{c_o/6}{1.5c_o}\right)$$

$$W = \frac{1}{2}\rho v^2 S_w Cl_w \left(1 - \frac{1}{6(1.5)}\right) = qS_w Cl_w (.89) \qquad \text{Eqn (3)}$$

Alternately, this means that the lift provided by the wing (WL) must be 12.5% greater than the aircraft gross weight.

4. Rationale for Tube-Spars

Hollow tubes were selected for both the fuselage and the wing spars for several reasons. Three major structural requirements were considered. They were: bending moments, buckling forces and torsion. Hollow tubes were not considered inherently superior to other possible spar shapes but in the fuselage spar it was the prospect of torsion between the propeller, wings and tail section that prompted a hollow tube. In the wingspars torsion was a consideration; however buckling loads were considered the principal structural consideration here. Hollow tubes were desireable for the streamlined effects of the leading edge in low-speed flight regimes. Overall, the choice of hollow tubes provided a versatile structural member for anticipated load conditions.

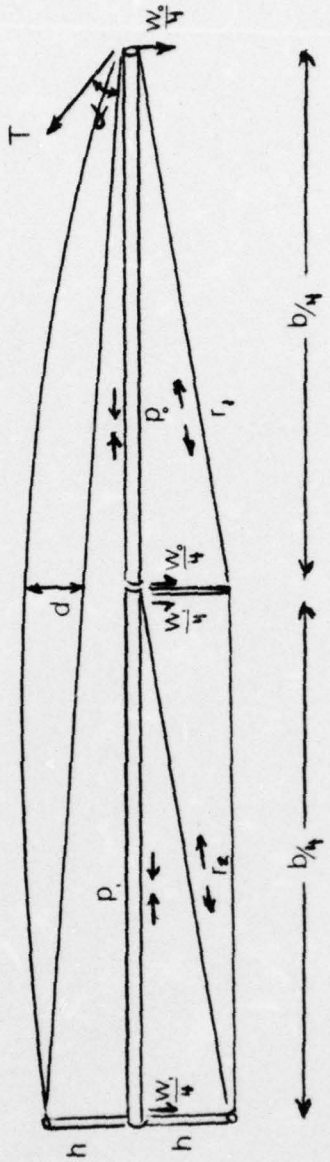

Figure 6 - WING SPAR COMPRESSIVE LOAD ANALYSIS

B. WING

1. Force Location and Identification

Wing spars were treated as columns for purposes of structural analysis. A schematic of compressive loading is shown in Figure 6. Compressive forces were observed in the outer wing spar due to the tension force from the jib and mainsail and from the outer restraining stay (R_1). Inner spar compressive loads were due to the total outer-spar compressive load plus a component from the inner restraining stay (R_2).

2. Wing-Spar Column Analysis

If the wingspar were to be subjected to a vertical distributed load from the mainsail as well as a compressive loading, then it would require analysis as a beam-column. This approach was not pursued for several reasons. First, as the subsequent tension analysis demonstrated, tensions in the sail were regarded as acting primarily in the spanwise direction. It was also intended that the mainsail was to carry no vertical loads in the coincident region of jib and mainsail. Finally, if some vertical loading were to result it could be disregarded in all probability according Ref 2:

> Since the critical load for the beam column is the same as the column critical load, it is apparent that the axial load which causes instability is independent of the lateral loads. This is true of all beam columns if none of the stresses exceeds the proportional limit.

All angles in Figure 6 were considered sufficiently small for small-angle approximations in analysis. The weight of the wing spars acting downward provided some assistance to the restraining stays in balancing the forces from the sail tension. Spar weights then aided in reducing

compressive forces within the spars due to the restraining stays. This fact further assisted in weight reduction. From statics and Figure 6:

at the wingtip

$$\Sigma Fy: \quad T\left(\alpha + \frac{h}{b/2}\right) = R_1\left[\frac{h}{b/4}\right] + \frac{W_o}{4} \qquad \text{Eqn (4)}$$

$$\Sigma Fx: \quad P_o = T + R_1 \qquad \text{Eqn (5)}$$

at midwing

$$\Sigma Fy: \quad R_1\left[\frac{h}{b/4}\right] = R_2\left[\frac{h}{b/4}\right] + \frac{1}{4}(W_o + W_i) \qquad \text{Eqn (6)}$$

$$\Sigma Fx: \quad P_i = P_o + R_2 \qquad \text{Eqn (7)}$$

for the critical compressive loading of a column as follows:

Eqn (8) $P_{cr} = \dfrac{c\pi^2 EI}{L^2}$ where c=end conditions

=1.0 pin ended, free
=2.04 pin ended, fixed
E=modulus of elasticity
I=moment of inertia
L=column length
r_o=outer radius
r_i=inner radius
t=wall thickness

for a hollow tube:

Eqn (9) $I = \frac{\pi}{4}(r_o^4 - r_i^4)$

$(r_o^2 + r_i^2)(r_o^2 - r_i^2)$

$(r_o^2 + r_i^2)(r_o + r_i)(r_o - r_i)$

for tubes with large radii compared to thickness $(r_o^2 + r_i^2)$ is approximately equal to $2r_o^2$, where $(r_o + r_i)$ approximately equals $2r_o$ and $(r_o - r_i) = t$. these approximations into equation (9) yielded:

$$I = \frac{\pi}{4}(r_o)^2 2r_o t = r_o^3 t\pi \qquad \text{Eqn (10)}$$

For an outer radius of 3.0 inches and a thickness of .03 inches this approximation compares as follows:

$$I = \frac{\pi}{4}(3.0^4 - 2.97^4) = 2.507 \text{ in}^4 \qquad \text{Eqn (9)}$$

$I=\pi(3.0)^3(.03)=2.545 \text{ in}^4$ Eqn (10)

(a difference of about 1.49%). Substituting equation (10) into equation (8), yields

Eqn (11) $P_{cr}=\frac{c\pi Er_o^3 t}{(b/4)^2}$ where:

r_o =outer radius

$b/4$=column length

This is the maximum compressive load that a column of given radius, thickness, length, specific end-conditions and type material can withstand.

3. Sail Tensions and Allowable Trailing-Edge Deflections

Reference 7 discussed circumferential stresses experienced in a thin-walled cylinder and was directly related to the sail tension equation development illustrated in Figure 7.

Eqn (12) $\sigma_\theta=\frac{Pr}{t_w}$ where σ_θ=circumferential stress in a thin-walled cylinder

P=pressure

r=cylinder radius

t_w =wall thickness

R=radius of curvature

σ_θ =wall tension unit area

$\sigma_\theta t_w$ =wall tension unit depth

Sail tensions were assumed to exist along the spanwise elements of a wing instead of in the chordwise direction. Consequently the force of the sail could be regarded as a series of tension strips running from root to tip with virtually nc fore-and-aft stress components. If the curvature of the trailing edge of the jib sail were regarded as a segment of a very

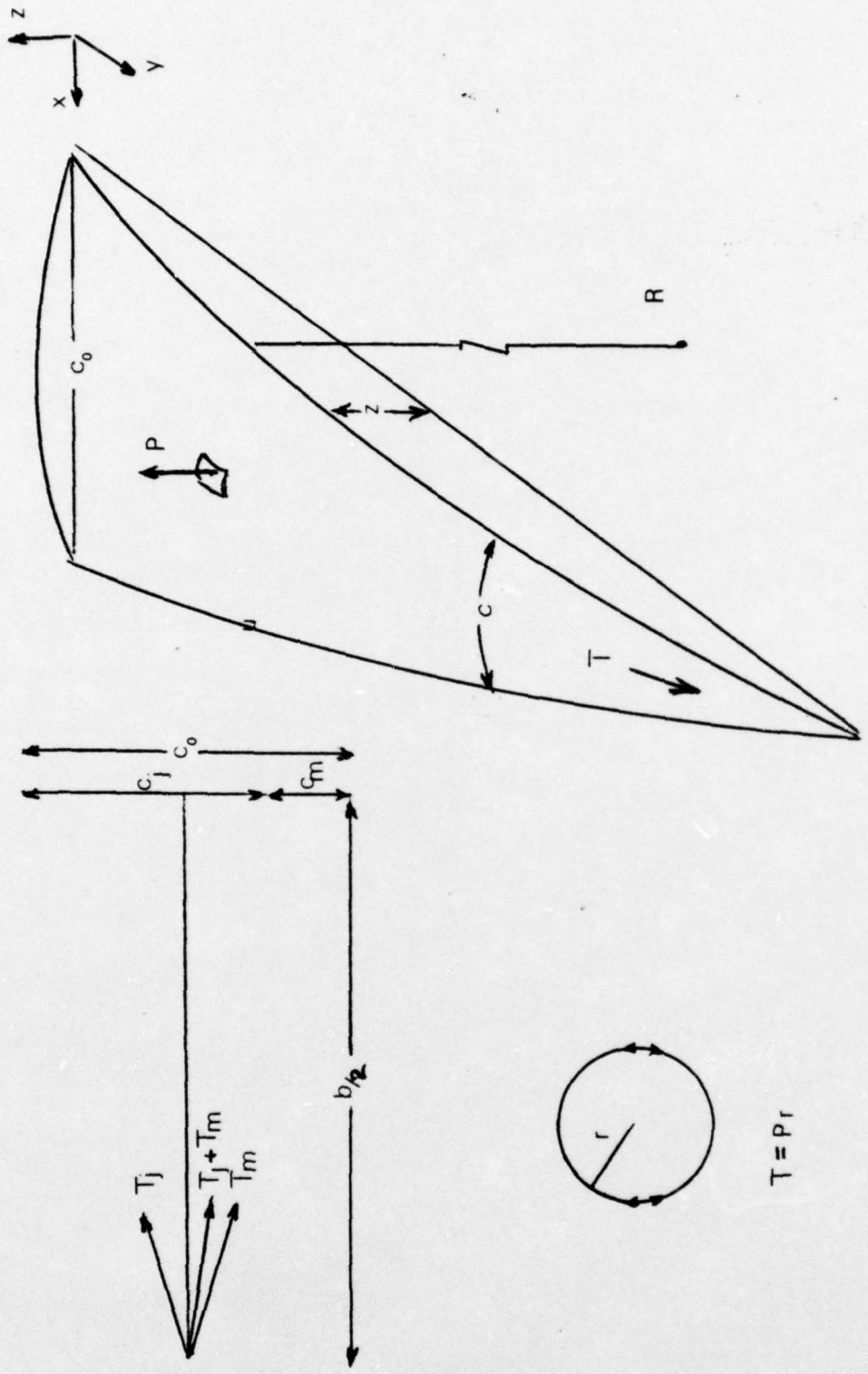

Figure 7 - ALLOWABLE DEFLECTIONS, TENSION BALANCE, AND THIN-WALLED CYLINDER

large circle, then the spanwise tension/unit chord (T/c=t) was equivalent to (t). Tension/unit chord was assumed to be a constant along each spanwise strip. In the small angle approximation the reciprocal of the sail radius of curvature was known to be equivalent to the second derivative of the deflection (z) with respect to spanwise position (y). These conditions modified Equation (12) to the following:

$$T/c=PR \qquad \text{Eqn (13}$$

For the jib sail:

$$\frac{1}{R}=\frac{d^2z}{dy^2}=\frac{Pc}{T_j}=-Pc_j\left(1-\frac{2y}{b}\right) \qquad \text{Eqn (14)}$$

where $c_j=c(1-2y/b)$

The negative sign originated from the radius of curvature orientation. Integrating equation (14) twice and solving for the constants of integration produced the following results:

$$\frac{dz}{dy}=\frac{Pc_j}{T_j b}\left(by-y^2\right)+A$$

$$z=\frac{Pc_j}{T_j b}\left(\frac{by^2}{2}-\frac{y^3}{3}\right)+Ay+B$$

with end conditions:

$$y=0,\ z=0 \qquad B=0$$

$$y=\frac{b}{2},\ z=0 \qquad A=\frac{Pc_j b}{6T_j}$$

Equation (14) then became an equation for the spanwise sail deflection:

$$z=\frac{Pc_j}{6T_j b}\left(2y^3-3by^2+b^2y\right) \qquad \text{Eqn (15)}$$

Solving Equation (15) for the spanwise deflection at midspan (y=b/4) resulted in

$$z = \frac{Pc_j}{64T_j}(2y^3 - 3by^2 + b^2y) \qquad \text{Eqn (16)}$$

While equation (16) provided a general expression for mid-span sail deflection, the maximum value (d) that the sail would be allowed to experience remained to be determined. It was assumed that mid-span deflection was directly proportional to the product of chord and a constant of proportionality (K_d). The equation indicated that the tension in the sail and the consequent design stay tensions and spar compressions increased linearly as the sail was drawn tighter and made flatter. This meant that there was a tradeoff between baggy sails and high loads. Judgement was exercised to allow the deflection to be limited to 5% of the root chord.

$$d = K_d c \qquad \text{Eqn (17)}$$

At midspan $d = K_d c_0/2$ Eqn(18). For a midspan deflection of 5% K_d became .10 Substituting Equation (18) into Equation (16) resulted in an expression for the required sail stay tension

$$T_j = \frac{Pc_j b^2}{64K_d c_0/2} = \frac{Pb^2 c_j}{32K_d c_0} \qquad \text{Eqn (19)}$$

But pressure (P) was equivalent to the total lifting force (WL) divided by the total wing area(S). Referring to Figure 6 it can be seen that the weight of the sails acts opposite to the lifting force. Since the sail supported its own weight plus the weight of the entire craft it was assumed that the weight of the sail should not affect Equation (19) and should therefore be deducted from the effect of the wing-lift:

$$T_j = \frac{(WL - \sigma_s S) b^2 c_j}{32K_d S c_0} = \frac{WL' b^2 c_j}{32K_d S c_0} \qquad \text{Eqn (20)}$$

For all considerations the area of the main sail directly beneath the jib was assumed to provide no lift. It was assumed that this region merely provided the slotted condition between the main and jib sails. Consequently for structural load considerations the main sail chord was measured from the trailing edge of the jib chord to the trailing edge of the main sail chord. Bearing this fact in mind a similar analysis of mainsail tensions lead to:

$$T_m = \frac{WL'b^2 c_m}{32K_d S c_o} \qquad \text{Eqn (21)}$$

The jib tension (T_j) and main tension (T_m) combined to equal the total tension (T) acting along the wing spar because $c_m + c_j = c_o$. Figure 7 shows a spanwise tension balance acting at one wingtip. When these forces and angles were summed, the result was a compressive force acting along the wing spar. Fore-and-aft force components were equal and opposite.

4. Location of the Center of Gravity

The mean aerodynamic chord of a triangular wing is located one-third the distance of the seni-span (b/6) from the fuselage. Therefore $c_{ave} = 2c_o/3$. The wing could also be regarded (Figure 8) to be a rectangular wing of the same span and two-thirds the value of the root chord. Stability considerations generally select the center-of-gravity location close to the quarter chord position. In this instance the quarter chord position of the equivalent rectangular wing can be seen to intersect the fuselage at a value one-third of the wing root chord.

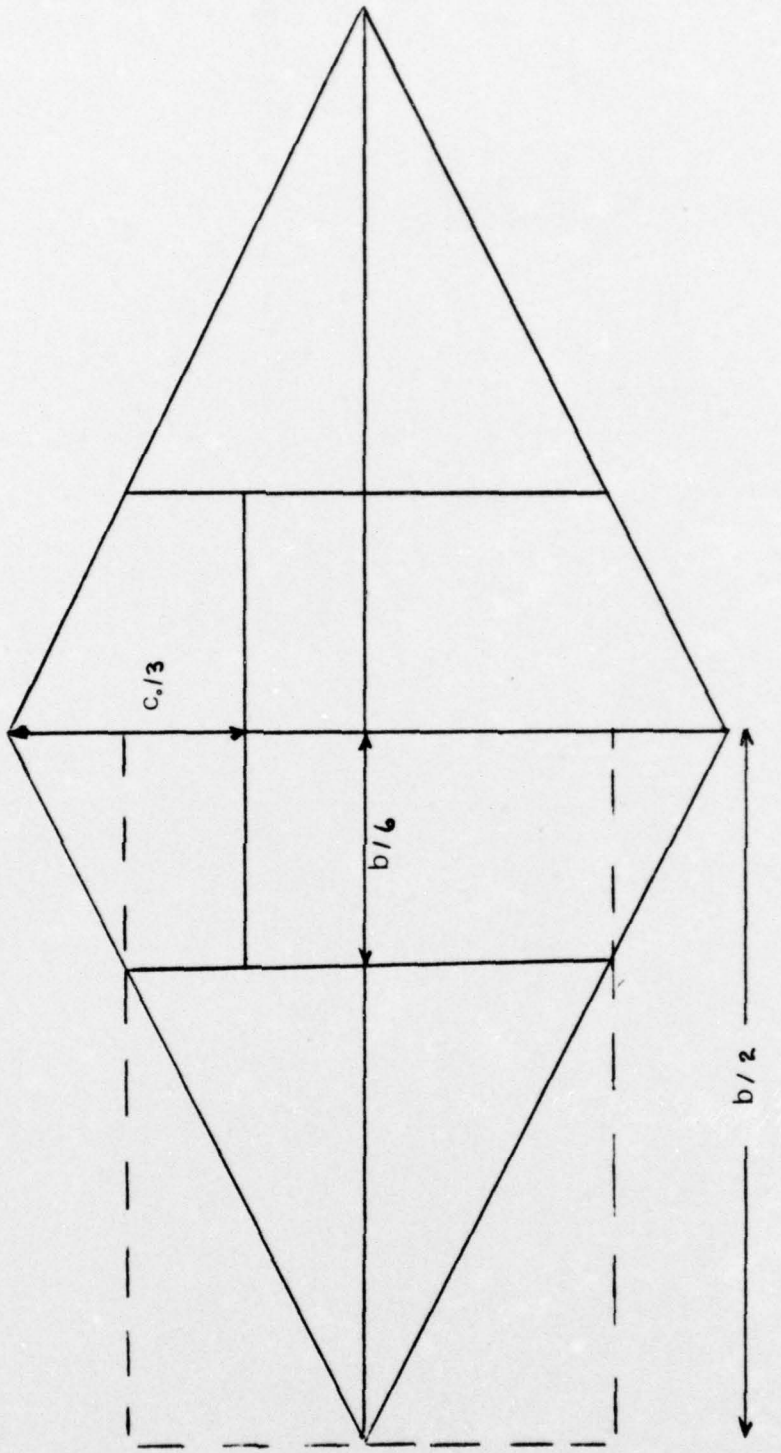

Figure 8 - SELECTION OF THE CENTER OF GRAVITY LOCATION

5. Initial Weight and Balance Caluclations

Several criteria were followed for initial weight and balance analysis:

a. Summation of Weight=Gross Weight (GW)

Gross weight included the initial weight estimates of:

$$GW=W=W_{body}+(W_{spars}+S)(1+K_t) \qquad \text{Eqn (22)}$$

where K_t=factor for the tail structure and was assumed to be 0.200.

b. Wing-Lift(WL) Equals the Gross Weight Plus the Absolute value of Tail Lift (TL)

The wing-lift must support not only the aircraft gross weight but also an additional amount equal to the tail lift loss as discussed in the Empennage Assumptions section.

$$\Sigma M_{cg}=0=qS_w Cl_w L_w - qS_t Cl_t L_t$$

$$S_w Cl_w L_w = S_t Cl_t L_t \qquad \text{Eqn (23)}$$

This substituted into Equation (22) yields an expression for weight and also wing-lift of the aircraft:

$$W=\frac{1}{2}\rho v^2 S_w Cl_w \left(1-\frac{L_w}{L_t}\right) \quad \text{where}$$

$$WL=\frac{W}{(1-L_w/L_t)}=\frac{1}{2}\rho v^2 S_w Cl_w \qquad \text{Eqn (24)}$$

c. Balance of Aerodynamic Forces

Aerodynamic forces must be balanced about the center-of-gravity as illustrated in Figure 4 Thus

$$WL(L_w)=TL(L_t) \qquad \text{Eqn (25)}$$

Due to the location of the center-of-gravity at one-third of the root chord aft of the leading edge and the wing-lift acting at the mid-point of the root chord, the value of "L_w" was found to be one-sixth of the root chord. "L_t" was assumed to be three-halves of the root chord value.

d. Weight and Balance

After the balance of aerodynamic forces was obtained, weight shifts were necessary to insure that the weights actually balanced at the center-of-gravity. The geometry of the aircraft was fixed with the exception of pilot location. Therefore all that remained was to position the pilot appropriately to bring the C.G. to the desired location. Care was required to insure that the propeller was further forward than the leading edge of the jib sail stay.

6. Spar Weights in Terms of Euler's Buckling Equation

A column subjected to compressive loads will fail when a critical load is reached or exceeded. Equation (11), was utilized for the development of wing spar weight expressions. Spar weight is equivalent to the material density times the volume of the structure. Spars are henceforth considered as "inner" spars and "outer" spars. For example, the weight of the outer spars is the weight of both outer wing spar segments. Thus

spar weight=density times volume= $2\pi rtb/2$ Eqn(26)

for an outer radius of 3.0 inches and a thickness of .03 inches this approximation compared as follows:

$$A_1=\pi(r_o^2-r_i^2)=(3.0^2-2.97^2)=.5626$$
$$A_2=2\pi rt=2\ 3.0\pi.03=.5655$$

(a difference of about 0.51%). Equation (11) may be rearranged to include spar weight terms as follows:

$$P_{cr} = \frac{c\pi^3 E r^3 t}{(b/4)^2} = \frac{c\pi^2 E r^2 (2\pi r t \rho b/2)}{(b/4)^2 \rho b}$$

$$P_{cr} = \frac{c\pi^2 E r^2 W}{(b/4)^2 \rho b} spar = \frac{16 c \pi^2 E (r/b)^2 W}{\rho b} spar \qquad \text{Eqn (27)}$$

While the distance in the numerator is a semi-span (b/2) for weight calculation, the denominator remains the length of each individual column (b/4) for buckling considerations. The weight of the wing spar is equivalent to the weights of the outer and inner wing spar sections. The (r/b) term was called the "slenderness ratio" and was one of the terms utilized in subsequent minimization analyses.

7. Compressive Load Analysis

Equations(4-7) state compressive loads in terms of aircraft geometry (Figure 6). The angle "alpha" was assumed to be equivalent to 2d/b/4. From the "allowable deflection" discussion $d=K_d c$. At midspan the chord value was half of the root chord and therefore $d=K_d c_o/2$. Looking at sail geometry $S=bc_o/2$ and therefore $d=K_d S/b$. Consequently $=8d/b=8K_d S/b^2$ Eqn (28). Solving Equation (4) for the tension force in the outer stay became

$$R_1 = \frac{WL'b^2}{32K_d S}\left[\frac{2K_d S}{bh} + \frac{1}{2}\right] - \frac{Wob}{16h} \qquad \text{Eqn (29)}$$

from Equation (5) the compressive loading in outer wing spars became

$$P_o = \frac{WL'b^2}{32K_d S}\left[\frac{2K_d S}{bh} + \frac{3}{2}\right] - \frac{Wob}{16h} \qquad \text{Eqn (30)}$$

Similarly from Equations (6) and (7) the following analysis was obtained for the inner wing spars:

$$R_2 = \frac{WL'b^2}{32K_d S}\left[\frac{2K_d S}{bh} + \frac{1}{2}\right] - \frac{b(2Wo+Wi)}{16h} \qquad \text{Eqn (31)}$$

$$P_i = \frac{WL'b^2}{32K_d S}\left[\frac{4K_d S}{bh} + 2\right] - \frac{b(3Wo+Wi)}{16h} \qquad \text{Eqn (32)}$$

8. Spar Weights in Terms of Buckling Criteria and Force Analysis

Euler's buckling equation provided an expression for the critical buckling load that may be applied to a column. It was then modified to reflect the weights of inner and outer wing spars (Equation 27). This set of equations was set equal to the compressive loads calculated from the aircraft geometry. Spar weights were calculated from these equations after the inclusion of a safety factor (SF) term, a universally accepted engineering practice. Equation (27) was thus modified to include a safety factor term in the denominator. When the safety factor exceeded its minimum value of 1.0, the resultant decrease in tolerable critical loading provided a margin of error. Thus, for the outer wing spars: $P_{cr_2} = P_o$ or

$$\frac{16c\pi^2 E(r_o/b)^2 Wo}{SF\ b^2} = \frac{WL'b^2}{32K_d S}\left[\frac{2K_d S}{bh} + 2\right] - \frac{Wob}{16h}$$

Solving for the weight of the outer spars (Wo) yielded:

$$Wo = \frac{WL'\left[1 + \frac{3bh}{4K_d S}\right]}{\left[1 + 16\frac{Z_o^2 Eh}{SF\rho b^2}\right]} \qquad \text{Eqn (33)}$$

where $Z_o = r_o/b$

For simplification of calculations let:

$$A = \frac{bh}{K_d S} \qquad B_o = \frac{16\pi^2 Z_o^2 Eh}{SF\rho b^2} \qquad B_i = \frac{16\pi^2 EZ_i^2 Eh}{SF\rho b^2}$$

then Equation (33) became

$$W_o = \frac{WL'(1+3A/4)}{(1+B_o)} \qquad \text{Eqn (34)}$$

Solving for W_i yielded

$$W_i = \frac{WL'[-1+2B_o+AB_o-5A/4]}{(1+2B_i)(1+B_o)} \qquad \text{Eqn (35)}$$

9. Total Weight and Wing-Lift/Unit Span Development

It was determined from Equation (2) that aircraft weight was equivalent to $WL(1-L_w/L_t)$. Aircraft gross weight was assumed to be a body weight (W_b), which was estimated in a previous section, plus the weight of the wing spars and sail, plus the empennage (assumed to weigh 20% of their respective wing components). Thus

$$W = WL(1-L_w/L_t) = W_b + (1+K_t)(W_{spars} + S) \qquad \text{Eqn (36)}$$

The combined weight of the wing spars became

$$W_{sp} = W_o + W_i = \frac{WL'[-A/2+2(B_o+B_i)+A(B_o+3B_i/2)]}{(1+2b_i)(1+b_o)} \qquad \text{Eqn (37)}$$

When this was substituted into Equation (36) an expression for wing-lift/unit span was obtained.

$$WL = \frac{\left[\frac{S}{1+K_t}\right]\left[\frac{W_b}{\sigma S} + \frac{1+K_t}{}\right] - \left[\frac{S\sigma[-A/2+2(B_o+B_i)+A(B_o+3B_i/2)]}{(1+2B_i)(1+B_o)}\right]}{b\left[\frac{(1-L_w/L_t)}{(1+K_t)}\right] - b\left[\frac{-A/2+2(B_o+B_i)+A(B_o+3B_i/2)}{(1+2B_i)(1+B_o)}\right]} \qquad \text{Eqn (38)}$$

Equation (38) represented the dominant term in the optimum power equation developed in a previous section.

Considerable attention was devoted towards minimizing its value.

10. Flexibility of Wing Sail Design

Two remaining terms in the optimum power equation that could be varied were the parasite drag area (f) and the wing efficiency factor (e). Both terms were examined for optimization possibilities. Aircraft wing geometry might be varied to improve the wing efficiency factor, referred to as Oswald's efficiency factor. One particularly attractive feature of Equation(38) is that it may be optimized independently from wing geometry. Conversely improvements in wing efficiency need not alter wing-lift/unit span calculations so long as wing area remained fixed.

C. POWER REQUIRED

Re-examining the power equation discussed in a previous section for drag terms evolved the following:

$$P = D V_1 \frac{\rho v^3}{2} S\left(Cd_p + \frac{Cl^2}{\pi A Re}\right) \qquad \text{Eqn (39)}$$

where the first term in parenthesis represented a parasite drag coefficient and the second term an induced drag. Certain assumptions as to their nature preceeded an examination of their minimization.

1. Parasite Drag Considerations

An equivalent parasite area (f) was obtained from the product of Cd_p and sail area S. This term was further broken down to a parasite drag for the man and fuselage (referred to as "f_{man}") and a term relating to the drag of the wing spars. Von Mises [Ref. 7] mentions a coefficient

of parasite drag "c_p," which is based on the frontal area of the body. Figure 9 [Von Mises 1959] presents a region of expected parasite drag coefficients for various geometries. The anticipated Reynolds number for man-powered-flight is on the order of 5.5×10^4.

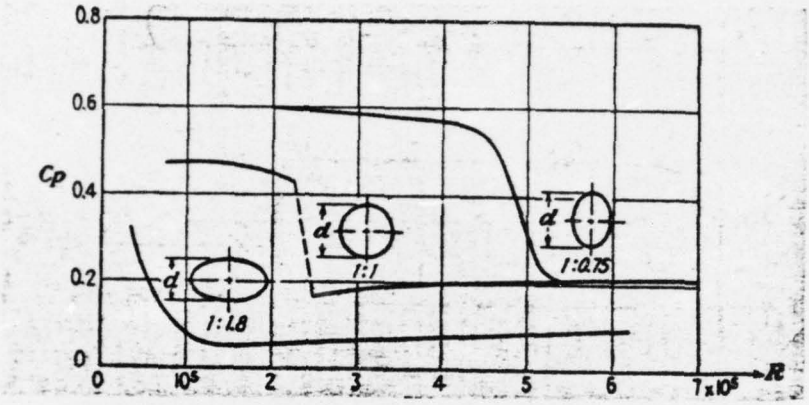

Figure 9-PARASITE DRAG COEFFICIENT Cp

The anticipated Reynolds number is on the lower extremity of this figure and suggests an increasing parasite drag coefficient value. However, a shape more streamlined than the ellipse was anticipated due to wrapping the sail about the wing-spar and reaffixing it to the mainsail some distance aft of the spar. A value of $c_p = .25$ was arbitrarily selected based on the above factors. A product of wing spar diameter times the wingspan yielded the frontal area mentioned earlier. The parasite area thus became

$$f = f_{man} + c_p (2r_o + 2r_i) b/2 \qquad \text{Eqn (40)}$$

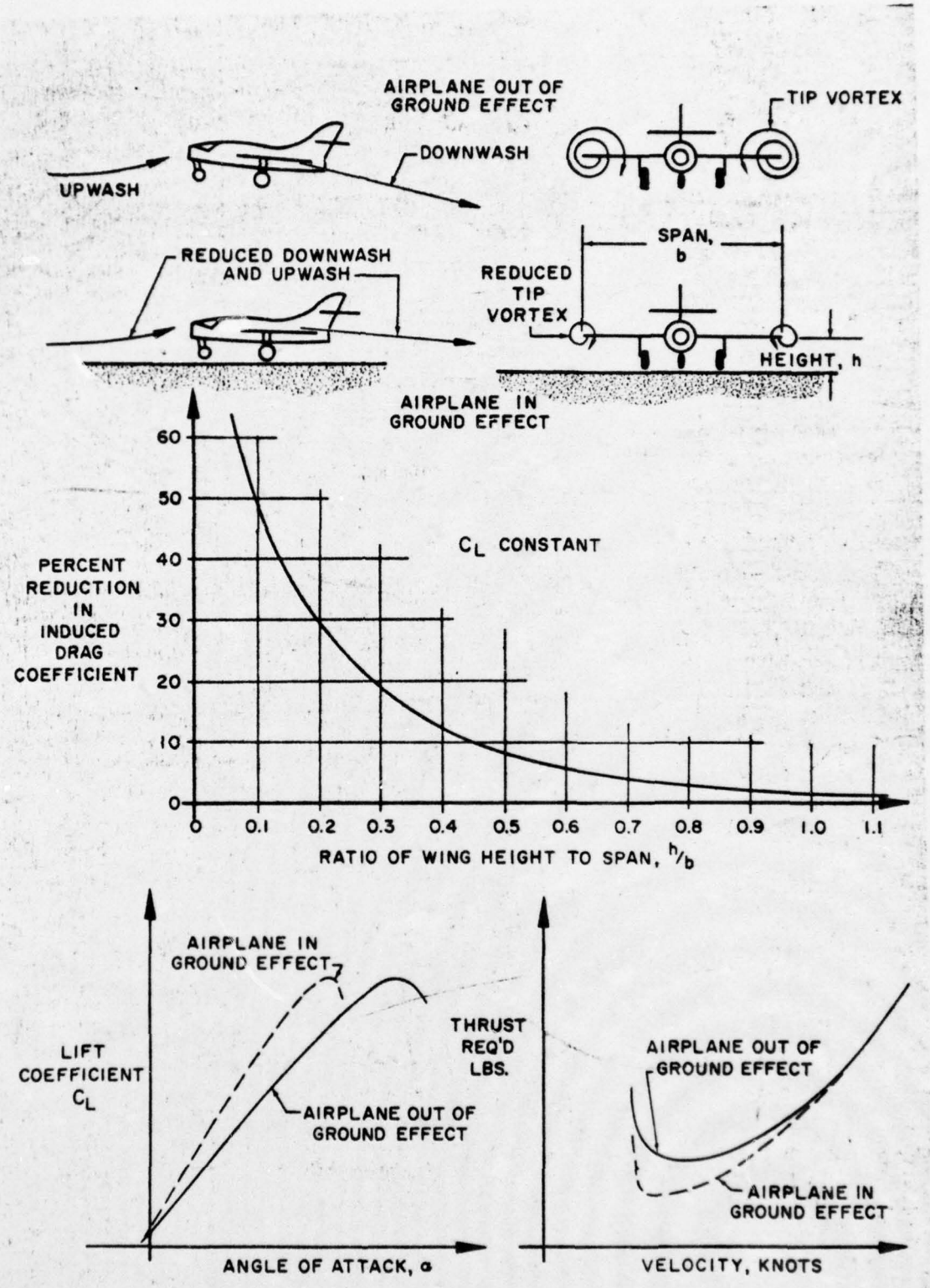

Figure 10 - GROUND EFFECT CONSIDERATIONS

2. Induced Drag Considerations

Induced drag (Cd_i) is equivalent to the square of the lift coefficient divided by the product of pi and the aspect ratio. Figure 10 shows a reduction in the induced drag and thrust required due to a phenomenon known as "ground-effect." Since the majority of the man-powered flight regime was expected to occur in close proximity with the earth, ground-effect provided an extremely useful drag reduction. With ground-effect the induced drag equation became

$$Cd_i = \frac{KCl^2}{\pi AR} \qquad \text{Eqn (41)}$$

where K represents a reduction due to ground-effect. Using the curve of Figure 10 and numerical approximation

h/b	%DEC C_{di}	K' (1-%)	Δ	Δ^2	Δ^3	Δ^4
0.1	.48	.52				
			.19			
0.2	.29	.71		-.09		
			.10		.05	
0.3	.19	.81		-.04		-.02
			.06		.03	
0.4	.13	.87		-.01		
			.05			
0.5	.08	.92				

INDUCED DRAG REDUCTION FORWARD INTERPOLATING POLYNOMIAL

Figure 11

techniques discussed in Gerald [Ref.1] a second order polynomial fit was obtained for induced drag reduction. Figure 11 illustrates the data employed for the drag reduction equation as a function of altitude/wing span

$$P_n(x) = K = fo + s\Delta fo + s\frac{(s-1)}{2!}\Delta^2 fo \qquad \text{where } s = \frac{x - .1}{.1}$$

$$K = .24 + 3.25x - 4.5x^2 \qquad x = h/b \qquad \text{Eqn (42)}$$

This equation enabled a quantitative analysis of induced drag reduction with altitude (for a given wing span).

D. SUMMATION

An equation for power was optimized in a previous section and yielded several variable terms. Of these WL/b was the dominant term and an equation for it was developed using the aircraft geometry and Euler's buckling equation. A parasite area term was identified and an expression developed based on the frontal area. Reductions in induced drag were noted due to ground-effect and the reduction was quantified according to a ratio of altitude divided by wing span. Oswald's wing efficiency was the last remaining variable and its improvement was cited as possible for a fixed sail area independent of the WL/b equation. Design modifications and optimization of the above factors were examined to bring the power required for flight within the attainable power available regime.

III. SEARCH FOR OPTIMUMS

A. COMPUTATIONAL ANALYSIS

The logical approach for further optimization at this point appeared to be similar to the optimization technique of the power equation from the Optimum Power section. Since the intention was to minimize the power-required, it followed that further optimization of the power equation was the obvious selection for further analysis and the development of an expression for WL/b was developed accordingly. The abbreviated terms in Equation (38) were expanded and it was intended to optimize this equation with respect to span just as the power equation had been optimized with respect to velocity. Setting the first derivation of Equation (38) equal to zero and solving for optimum span resulted in a tenth order equation in terms of span. Further efforts at optimization through this technique were abandoned and an extensive analysis of optimization through a digital computer approach was selected.

B. COMPUTER ANALYSIS

1. "Plot P" Optimization

The first computer program developed was called "Plot P" because of the subroutine employed for graphical output of WL/b. It was felt that there would be an optimum value of WL/b for a given set of inputs as the span was

allowed to vary. The required inputs to this program included the constants K_d, K_t, h, T_t, and sail weight/unit area. Also required were the variable terms "Q" (the inverse of the inner slenderness ratio) which was a more convenient numerical expression than the slenderness ratio itself; "X" which was a ratio of the outer/inner spar radii, and "S" the sail area. Plots of WL/b vs. b produced a mimimum for each choice of the parameters Q,X,and S. The analysis then became a systematic examination of these combinations for an overall minimum.

2. "Tab" Outputs

The "Tab" program was created to produce a tabulation of the parameters chosen above and the results that were obtained. Input data included the same information as required by "Plot P" plus the estimated body weight (W_b) and the optimum wingspan indicated by the "Plot P" program. The critical factors in the "Tab" program output reduced to the inner and outer wing spar thicknesses, the lift coefficient and the calculated power required. Other output provided trend comparisons, spar radii, spar weights, overall weights etc. The combination of these computer programs enabled a systematic examination of the variables Q,X, and S for the best possible combinations to minimize Equation (38) while remaining within the established limitations.

3. Variation of Parameters

Figure 12 illustrates the trend in WL/b caused by separately increasing each of the parameters. It suggested improvements in WL/b from increasing sail area, increasing spar radii and from the outer spar radii

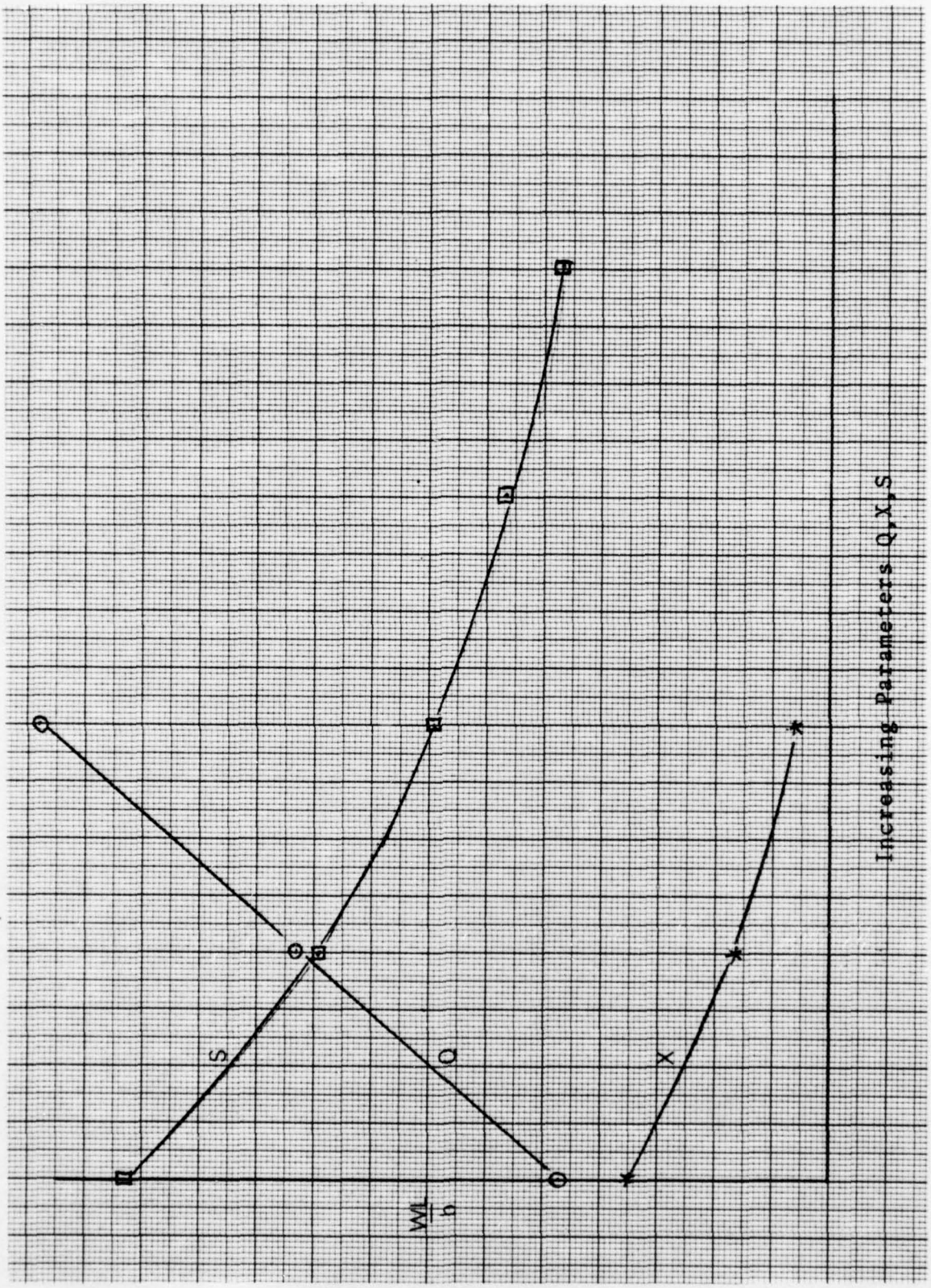

Figure 12 - GRAPHICAL EFFECT OF VARIATION OF PARAMETERS

being larger than the inner ones. Increasing spar radii resulted in decreasing spar thicknesses and consequent weight and power reductions. Larger outer spars were attributed to the differences in respective spar end conditions as noted in the wing-spar column analysis. It seemed reasonable that a pin-ended column would require a larger radius than a fixed-ended column to successfully withstand buckling loads. While this configuration might present a slightly unorthodox appearance it was considered desireable from a design standpoint Figure 13 shows the parameter influences in broader terms. Data for both Figures 12 and 13 were obtained from the "Tab" and "Plot p" computer programs. Once the wing spar thickness had been chosen, the Q and X parameters were adjusted to attain computed spar thicknesses as near to .030" as possible in both inner and outer spars. This procedure was repeated for sail areas ranging from 500 to 1500 square feet. Spar thicknesses equal to .030"±.001" under various conditions. Wing spars were the optimum spans indicated from "Plot p" computer output. WL/b, t_i, t_o, Cl, and power (including ground effects) were calculated by "Tab." Having satisfied the spar thickness criteria, the lift coefficients and power required values were examined. All power values appeared to

	WL/b	P_g	b	t_i	t_o
↑S	↓	↓	↑	↓	↓
↑Q	↑	↑	↓	↑	↑
↑X	↓	↓	↑	↑	↓

Figure 13 EFFECTS OF SEPARATE VARIATION OF PARAMETERS

be within a feasable range as did most of the lift coefficients. It appeared at this point that further improvement in WL/b could only be achieved through an increase in Oswald's efficiency factor, a decrease in the parasite drag or a reduction in the body weight. The latter had been only a first approximation and not yet the subject of detailed examination. Fuselage spar weights were calculated using a third computer program which also calculated weight and balance information, as well as shear and bending stresses in the fuselage spar. Because the program also dealt with different sail shapes the entire discussion was treated in a subsequent section.

C. TRADE-OFF ANALYSIS

Several options remained available at this point which might serve to increase the power available (2-man crew), decrease the aircraft weight (lighter construction materials) or increase the wing efficiency (wing shapes other than pointed wingtips). In addition, the parasite drag and sail weight sensitivities were examined. Computer output lists comparisons of various trade-off considerations.

1. Two-Man Crew

The idea of a two-man crew was entertained briefly. Its attractive feature was a doubling of the power available to propel the craft. As indicated by the optimum power equation, however, the relationship between power-required and weight was not a linear one. The geometric penalties incurred from another crewman more than offset the linear increase in power available. Thus a single-piloted craft was selected relatively early in the study and the multi-piloted version was not considered further.

2. Magnesium versus Aluminium

Magnesium was considered as a structural alternative to aluminium principally because of its significant decrease in density. At the same time there was also a decrease in the Modulus of Elasticity (a measure of a material's stiffness) which might adversely affect the structural integrity of the craft. Also allowable shear and bending stresses were lower. "Plot P","Tab" and "Wt-Balance" programs were run using magnesium's properties and the results compared to aluminium. Equivalent spar thicknesses in both metals required larger magnesium spars (lower Q and larger X) and slightly longer optimum wing spans were indicated. It appeared that a decreased modulus of elasticity dictated an overall increase in spar size. Improvements in magnesium spar weights were offset by the larger and heavier fuselage spar. The shear and bending stresses appeared to be critical factors in magnesium. An interesting combination might include an aluminium fuselage with magnesium wing spars. Further investigation of the magnesium option is warranted concerning maximum shear and bending stresses.

Aluminium was considered the superior selection based on the above analysis. It had the additional advantages of availability and lower costs.

3. Parasite Drag Sensitivity

In order to assess parasite drag influences on the power required, the value of "f_{man}" was set to zero. This drag modification was introduced into the "Tab" computer program and its results compared with a run in which $f_{man}=3.5$ ft^2 as originally assumed. For the 1000 foot sail area the power required dropped from .345 to .325

horsepower. In otherwords a complete elimination of the f_{man} drag term yielded a reduction in power-required of approximately 6%. This confirmed earlier suspicions concerning the drag variable as a fairly insensitive factor. Efforts directed at enclosing the pilot in a streamlined fuselage would not eliminate f_{man} and could be costly in terms of increased weight.

4. Sail Weight Sensitivity

Original conceptions for sail weights consisted of the lightest dacron material available. Dacron was considered preferrable to nylon because of the former's resistance to stretch under loaded conditions. A weight figure of 3/4 ounce per square yard was provided by commercial sources and was utilized in early sail weight calculations. Later, information from Sailrite Kits, a firm dealing in do-it-yourself sails, indicated that 2.2 ounce dacron might be the lightest obtainable and that this figure was for a 36"x 28.5" section. This revised sail weight was introduced into the "Tab" computer program to examine its effect on power requirements. Not surprisingly the greatest deviations were noted in the larger sail areas with the range of deviations running from a low of about a 4% power required increase to 10% on the 1500 square foot sail. The 1000 square foot sail required about an 8% increase (.317 vs .345 hp). Thus, a rather dramatic increase in the weight of the sail material was not catastrophic to the overall performance requirements. It did however, indicate that lighter sails would be strongly preferrable to the 2.2 ounce case. Further, while the 1000 square foot sail area was clearly superior for the lighter sail, a 750 square foot sail would be equally effective in the heavier instance.

The latter assumed that the higher lift coefficient was acceptable.

5. Taper-Ratio versus Pointed Wingtip

Oswald's efficiency includes the products of the planform efficiency (which is 1.0 for elliptical wings), body interference effects, separation and stall effects, tail contributions, propeller effects, flap effects etc. Experience has shown that an Oswald efficiency of 85% is about the best that an elliptical wing can hope to obtain. Further decreases occur as wing shape is modified. In practice elliptical wing construction is a difficult matter and truly elliptical wings are rarely built. Approximations to an elliptical wing can be obtained by a wing with a finite wingtip chord. Glauert Ref '3" has shown the effects of wing taper ratio (wingtip chord divided by wing root chord) on fractional drag increase over an elliptical wing (Figure 14) From aerodynamics $Cd_i = C_l^2 / \pi AR e$ and therefore

$$e = \frac{Cl^2}{\pi AR Cd_i} \qquad \text{Eqn (43)}$$

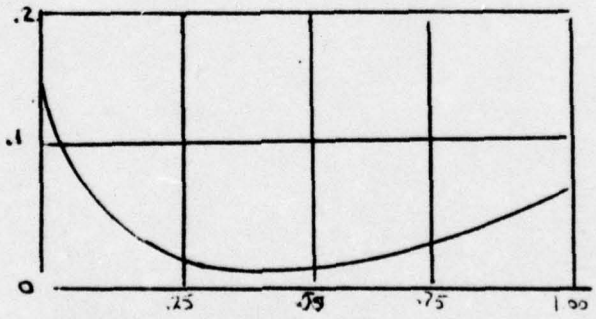

Figure 14. TAPER RATIO EFFECTS ON DRAG INCREASE

It was apparent that some benefit could be gained from using a tapered airfoil over a pointed wingtip. The question

posed a tradeoff between a weight increase from the additional wingtip boom requirements versus anticipated gains in wing efficiency. The wingtip boom would have to sustain bending moments from the lifting force of the sails. With this consideration in mind a taper ratio of 20% was selected as still having a favorable reduction in drag while also providing a small tip chord. Smaller tip chords would decrease the bending moments with consequent weight savings in the wingtip boom. A computer program was created to examine this question and its description follows.

a. "Weight-Balance" Computer Program

This program was initially created to solve the weight-and-balance question relating to pilot and propeller positioning. It was expanded to calculate a fuselage weight based on shear and bending stresses and further expanded to examine a wingtip boom in a similar manner. Inputs required from the "Tab" computer program included the computed spar weights and the wing-lift, and from "Plot P" the optimum span. In addition the same assumptions were required plus any desired wing taper ratio. Outputs included the positioning of the man and propeller, size and weight of the fuselage spar, sail dimensions, an accurate body weight and the size and weight of the wingtip boom. Shear and bending stresses were also listed as a matter of interest. Maximum shear and bending values were obtained from Ref '5" using a yield stress for a hollow tube (good for thicknesses up to .249 inches). Ref '5" further indicated that "compressive yield stress was approximately the same as tensile yield stress" for this case.

Optimum parameter cases with sail areas ranging from 500-1500 square feet were examined with detailed analysis on the 1000 square foot sail. In this instance arbitrarily selected fuselage radii of 2" and 3" were examined with each of these considered for tapered and pointed wingtips. The smaller fuselage spar radius was

found to be adequate in terms of the stress analysis and preferrable in terms of weight savings. Tapered wings produced lighter and smaller fuselage spars because the root chord was reduced and many assumptions on fuselage length were in terms of the root chord. A weight penalty of three pounds for both wingtip booms for the 1000 square foot sail appeared to be well within acceptable weight penalty limits. A rough estimate of drag decrease was obtained from Figure 9 comparing a pointed wingtip with a 20% taper ratio and both of these to an elliptical wing. The curve peaked on the left side of the curve at about 13% . This was subtracted from the 85% efficiency of the elliptical wing and for pointed wingtips an efficiency of 70% was used in calculations. For the tapered wingtip estimates yielded (1.13-1.04)/1.13=.0796, or roughly an 8% drag reduction over the pointed wingtip. Then .0796 times .08 yielded about 5% improvement. Values of .75 were used for the tapered wings. Since induced drag and wing efficiency were seen to be inversely proportional from Equation (43), then a 5% reduction in induced drag might suggest a 5% increase in wing efficiency. Improved wing efficiencies were introduced into "Tab" to examine the effects of improved wing efficiency versus a wingtip boom weight addition. Results indicated an decrease in power-required of approximately 6% for the 1000 square foot sail and slightly less improvement in others. It was therefor concluded that the tapered wing was a desireable option due to the decreased power requirements despite the increase in weight and structural complexity.

D. AREAS FOR FURTHER CONSIDERATION

While the structural design of the craft had been determined at this point several areas worthy of further consideration exist and exploration would be desireable, if

not essential, prior to actual flight testing such a craft.

1. Propeller Optimization

Given the human capacity for sustained power output an analysis of the optimum RPM and propeller blade diameter would enable an increase of the power efficiency. The power efficiency for all calculations thus far was chosen to be .8 . Naturally any improvement in this would further decrease power requirements. Reference '8" discusses this problem in depth. Due to the design of the aircraft to this point a propeller diameter of approximately eight feet appeared to be about a maximum. From Sherwin's '8" figure reproduced below an rPM of about 250 would yield a propeller efficiency of better than 85%. This would be a significant addition to the improvement of the propulsion efficiency.

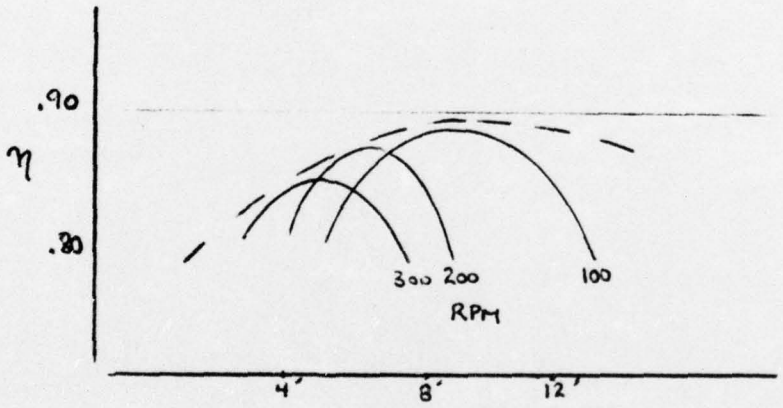

Figure 15

PROPELLER EFFECTIVENESS WITH VARIATION OF LENGTH AND RPM

2. Stability and Control

Little attention had been accorded the actual control problem of the aircraft and its gust response would have to be analysed in some detail. Flutter problems would need to be addressed as well. Since the aircraft was essentially two large moments of inertia (wing and horizontal tail) there remained a question of torsion due to gusts and asymmetrical lifting forces from the wings. If a wake disturbance from the wing arrives at the tail in a time comparable to the time for one cycle of a torsional oscillation between wing and tail then flutter instability can develope. Further restraining stays would be essential to eliminate this problem. Finally a small prototype should be constructed to examine the validity of all assumptions and the control responses necessary. In addition, uncertainties as to the sail's actual performance remain to be resolved.

IV. CONCLUSIONS

The concept of a sail-wing and exposed structure appeared to produce a vehicle possessing performance characteristics competitive with conventional rigid-wing designs. However ,while the optimum power equation indicated areas for optimization analysis, man-powered flight is impossible without ground effects.

For each sail area selected an optimum combination of wing and fuselage size and shape existed. Principal improvements were seen to be in the area of weight reduction although other refinements were beneficial. It appeared that a light sail, tapered wing and magnesium wing spars with an aluminium fuselage spar would give the highest performance for a sail-wing type of aircraft.

While many details of construction engineering have not been examined, indications are that the aircraft flying at Kitty Hawk might ave been closer to a successful man-powered prototype than anything that has yet followed.

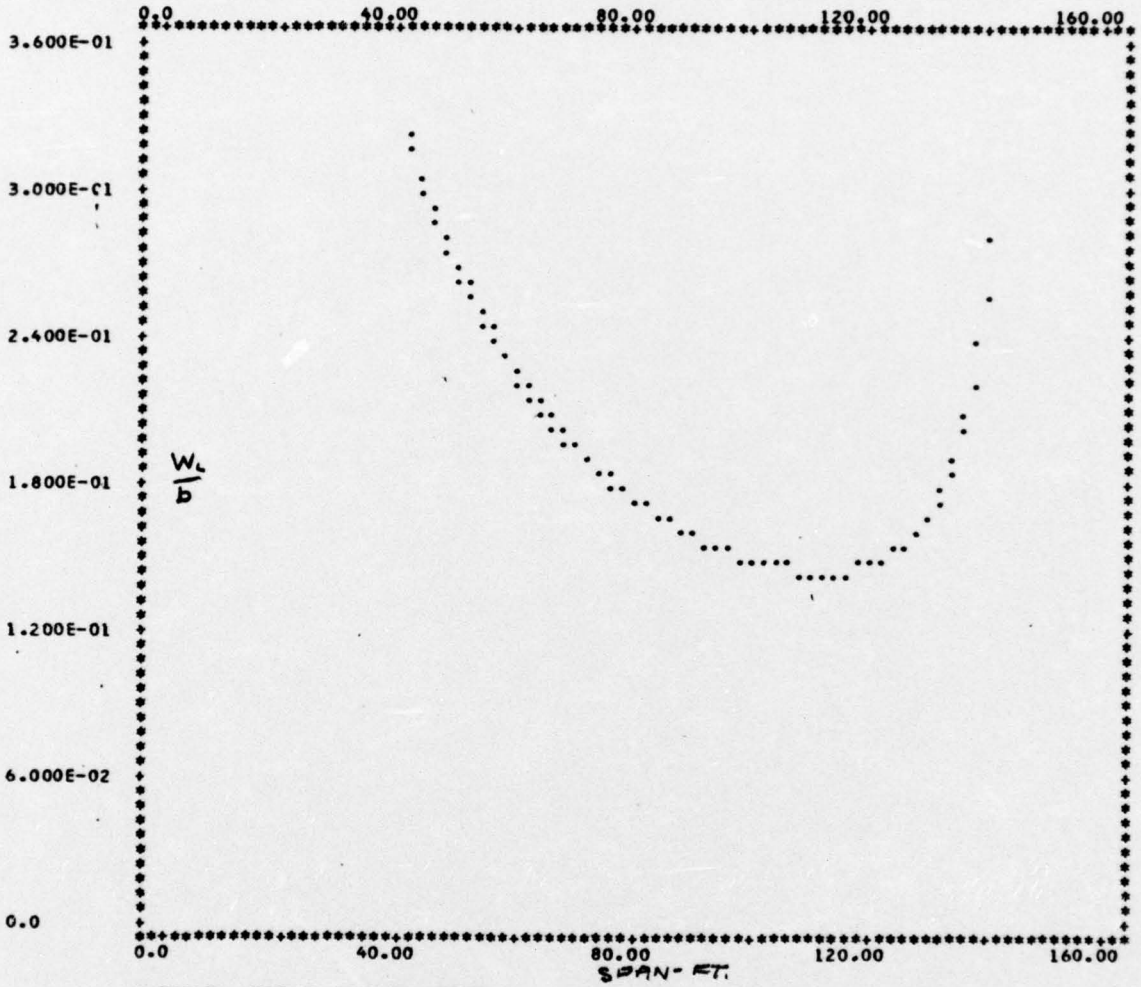

X-SCALE: "*"= 0.200E 01 UNITS

Y-SCALE: "*"= 0.600E-02 UNITS

PLOT OF WL/B VS B Q=376. X=1.12 SF=1.5

ASSUMPTIONS

FT2	LB/FT2	LB	FT			
500.	.01930	0.	4.	.20	.10	1.5
SAIL	SIGMA	WB	H	KT	KD	L

DATA IS TABULATED USING ALUMINIUM COMPONENTS

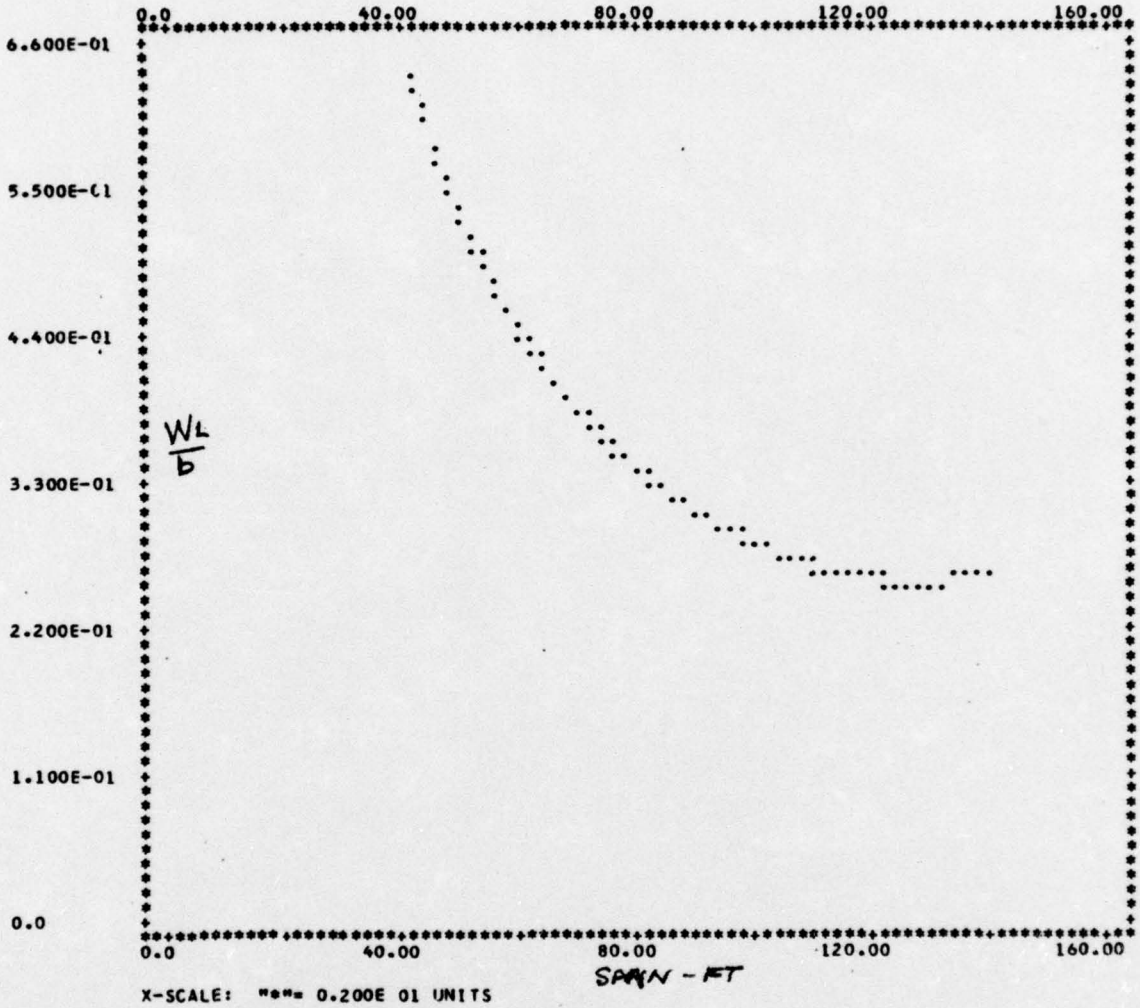

X-SCALE: "*"= 0.200E 01 UNITS

Y-SCALE: "*"= 0.110E-01 UNITS

PLOT OF WL/B VS B Q=423. X=1.11 SF=1.5

ASSUMPTIONS

FT2	LB/FT2	LB	FT			
1000.	.01930	0.	4.	.20	.10	1.5
SAIL	SIGMA	WB	H	KT	KD	L

DATA IS TABULATED USING ALUMINIUM COMPONENTS

REFERENCE

COMPUTER VARIATIONS					WEIGHT ANALYSIS				STRUCTURAL ANALYSIS						FLIGHT ANALYSIS 1 MILE FIG.8					
FT**2			FT		TOTAL	FUSE	SPARS		LBS		INCHES		INCHES		HP	FT/S			SEC	P(GE)
S	B/RI	X	SPAN	WL/B	WL	WB	WI	WO	PI	PO	RI	RO	TI	TO	P(R)	V	CL	AR	T.O.F.	HP
500.	375.	1.13	93.	3.701	343.9	211.	34.	37.	4367.	3136.	3.0	3.4	.0303	.0308	0.86	17.2	1.95	17.3	457.1	0.352
750.	402.	1.11	98.	3.630	357.6	216.	34.	38.	3604.	2551.	2.9	3.3	.0291	.0307	0.84	16.9	1.40	12.9	465.8	0.345
1000.	421.	1.11	104.	3.563	375.1	220.	37.	40.	3328.	2333.	3.0	3.3	.0291	.0304	0.84	16.6	1.15	10.9	475.0	0.345
1250.	441.	1.13	108.	3.704	400.0	231.	40.	41.	3183.	2209.	2.9	3.3	.0309	.0303	0.89	16.7	0.96	9.3	471.4	0.364
1500.	449.	1.12	110.	3.873	426.0	246.	41.	43.	3076.	2111.	2.9	3.3	.0310	.0308	0.96	16.9	0.83	8.1	465.7	0.393

DATA IS TABULATED USING ALUMINIUM COMPONENTS, SF=1.5, TAPERED WING WITH CT/CO=.2, EFF=.75 2.2 OZ SAIL
GROUND EFFECT COMPUTATIONS USING ALTITUDE=10% OF B

ASSUMPTIONS

SIGMA LB/FT2	WB LB	H FT	KT	KD	L
.01930	246.	4.	.20	.10	1.5

MAGNESIUM

COMPUTER VARIATIONS					WEIGHT ANALYSIS				STRUCTURAL ANALYSIS						FLIGHT ANALYSIS 1 MILE FIG.8					
FT**2			FT		TOTAL	FUSE	SPARS		LBS		INCHES		INCHES		HP	FT/S			SEC	P(GE)
S	B/RI	X	SPAN	WL/B	WL	WB	WI	WO	PI	PO	RI	RO	TI	TO	P(R)	V	CL	AR	T.O.F.	HP
500.	343.	1.13	86.	3.644	312.1	215.	21.	22.	3466.	2455.	3.0	3.4	.0309	.0309	0.84	17.1	1.80	14.7	460.8	0.344
750.	357.	1.13	98.	3.567	347.9	229.	26.	27.	3496.	2450.	3.3	3.7	.0309	.0306	0.85	16.1	1.50	12.7	488.1	0.349
1000.	366.	1.13	103.	3.726	385.6	251.	28.	30.	3444.	2382.	3.4	3.8	.0309	.0302	0.93	16.1	1.25	10.7	488.2	0.382
1250.	372.	1.12	103.	4.164	428.1	285.	28.	29.	3249.	2203.	3.3	3.7	.0309	.0304	1.10	17.0	1.00	8.5	463.3	0.452
1500.	381.	1.11	103.	4.374	450.1	300.	27.	28.	3032.	2025.	3.2	3.6	.0310	.0308	1.19	17.4	0.89	7.1	452.8	0.487

DATA IS TABULATED USING MAGNESIUM COMPONENTS, SF=1.5, TAPERED WING WITH CT/CO=.2, EFF=.75 2.2 OZ SAIL
GROUND EFFECT COMPUTATIONS USING ALTITUDE=10% OF B

ASSUMPTIONS

SIGMA LB/FT2	WB LB	H FT	KT	KD	L
.01930	300.	4.	.20	.10	1.5

POINTED WINGTIP

COMPUTER VARIATIONS					WEIGHT ANALYSIS				STRUCTURAL ANALYSIS						FLIGHT ANALYSIS 1 MILE FIG.8					
FT**2			FT		TOTAL	FUSE	SPAPS		LBS		INCHES			INCHES	HP	FT/S			SEC	P(GE)
S	B/RI	X	SPAN	WL/B	WL	WB	WI	WO	PI	PO	RI	RO	TI	TO	P(R)	V	CL	AR	T.O.F.	HP
500.	375.	1.13	93.	3.678	341.7	210.	33.	36.	4339.	3116.	3.0	3.4	.0301	.0306	0.90	17.5	1.88	17.3	450.7	0.367
750.	403.	1.11	99.	3.630	357.8	216.	34.	38.	3608.	2554.	2.9	3.3	.0292	.0308	0.89	17.2	1.35	12.9	457.7	0.363
1000.	423.	1.11	105.	3.557	371.8	217.	37.	40.	3304.	2317.	3.0	3.3	.0292	.0305	0.87	16.8	1.11	10.9	468.9	0.357
1250.	443.	1.13	108.	3.657	395.7	227.	40.	42.	3153.	2189.	2.9	3.3	.0310	.0304	0.92	16.9	0.93	9.4	465.9	0.375
1500.	451.	1.12	110.	3.813	420.2	241.	41.	43.	3036.	2085.	2.9	3.3	.0309	.0308	0.99	17.1	0.81	8.1	460.9	0.404

DATA IS TABULATED USING ALUMINIUM COMPONENTS, SF=1.5 FMAN=3.5 POINTED WINGTIP(EFF=.7), 2.2 OZ SAIL
GROUND EFFECT COMPUTATIONS USING ALTITUDE=10% OF B

ASSUMPTIONS

SIGMA LB/FT2	WB LB	H FT	KT	KD	L
.01930	241.	4.	.20	.10	1.5

$f_{man}=0$

COMPUTER VARIATIONS					WEIGHT ANALYSIS				STRUCTURAL ANALYSIS						FLIGHT ANALYSIS 1 MILE FIG.8					
FT**2			FT		TOTAL	FUSE	SPARS		LBS		INCHES		INCHES		HP	FT/S			SEC	P(GE)
S	B/RI	X	SPAN	WL/B	WL	WB	WI	WO	PI	PO	RI	RO	TI	TO	P(R)	V	CL	AR	T.O.F.	HP
500.	375.	1.13	93.	3.701	343.9	211.	34.	37.	4367.	3136.	3.0	3.4	.0303	.0308	0.81	18.4	1.71	17.3	428.8	0.330
750.	402.	1.11	98.	3.630	357.6	216.	34.	38.	3604.	2551.	2.9	3.3	.0294	.0307	0.79	18.0	1.24	12.9	438.1	0.325
1000.	421.	1.11	104.	3.593	375.1	220.	37.	40.	3328.	2333.	3.0	3.3	.0291	.0304	0.79	17.6	1.02	10.9	448.5	0.326
1250.	441.	1.13	108.	3.704	400.0	231.	40.	41.	3183.	2209.	2.9	3.3	.0309	.0303	0.84	17.7	0.86	9.3	445.9	0.344
1500.	449.	1.12	110.	3.873	426.0	246.	41.	43.	3076.	2111.	2.9	3.3	.0310	.0308	0.91	17.8	0.75	8.1	441.6	0.372

DATA IS TABULATED USING ALUMINIUM COMPONENTS, SF=1.5, TAPERED WING WITH CT/CO=.2, EFF=.75 2.2 OZ SAIL FI
GROUND EFFECT COMPUTATIONS USING ALTITUDE=10% OF B

ASSUMPTIONS

SIGMA LB/FT2	WB LB	H FT	KT	KD	L
.01930	246.	4.	.20	.10	1.5

215

3/4 oz SAIL

COMPUTER VARIATIONS					WEIGHT ANALYSIS				STRUCTURAL ANALYSIS						FLIGHT ANALYSIS 1 MILE FIG.8					
FT**2			FT		TOTAL	FUSE	SPARS		LBS		INCHES		INCHES		HP	FT/S			SEC	P(GE)
S	B/RI	X	SPAN	WL/B	WL	WB	WI	WO	PI	PO	RI	RO	TI	TO	P(R)	V	CL	AR	T.O.F.	HP
500.	375.	1.13	93.	3.589	333.4	211.	33.	36.	4323.	3104.	3.0	3.4	.0300	.0305	0.82	17.0	1.95	17.3	464.2	0.336
750.	404.	1.11	99.	3.481	343.4	216.	34.	38.	3573.	2530.	2.9	3.3	.0291	.0307	0.79	16.6	1.40	13.0	475.3	0.324
1000.	423.	1.11	105.	3.404	356.1	220.	37.	40.	3289.	2307.	3.0	3.3	.0291	.0305	0.78	16.2	1.15	10.9	487.5	0.318
1250.	444.	1.13	108.	3.476	376.3	231.	40.	42.	3139.	2180.	2.9	3.3	.0309	.0304	0.81	16.2	0.96	9.4	486.1	0.330
1500.	452.	1.12	110.	3.601	397.1	246.	41.	42.	3022.	2076.	2.9	3.3	.0309	.0308	0.86	16.3	0.83	8.1	482.4	0.352

DATA IS TABULATED USING ALUMINIUM COMPONENTS, SF=1.5, TAPERED WING WITH CT/CO=.2, EFF=.75 3/4 OZ SAIL
GROUND EFFECT COMPUTATIONS USING ALTITUDE=10% OF B

ASSUMPTIONS

SIGMA LB/FT2	WB LB	H FT	KT	KD	L
.00521	246.	4.	.20	.10	1.5

MAGNESIUM

MAGNESIUM STRUCTURE BASED ON MAX BENDING=26KSI,MAX SHEAR=19KSI, SHEAR AND BENDING STRESSES IN PSI, T,R, IN INCHES

		FUSELAGE SPAR				SAIL DATA			WEIGHT DATA					COMPUTED STRESSES		WINGTIP SPAR				COMPUTED STRESS	
X	Y	LENGTH	T	R	CO	CT	AREA	SPAN	BODY	WFUSE	WSPARS	A/C		BENDING	SHEAR	WEIGHT	LENGTH	T	R	BENDING	SHEAR
1.28	2.00	17.49	.04	2.0	9.5	1.89	500.	88.	215.	9.3	45.0	100.		24217.	2442.	3.3	1.9	.12	1.0	25739.	8305.
2.51	2.00	23.07	.06	2.0	12.4	2.48	750.	101.	229.	19.4	56.0	133.		24336.	1554.	5.5	2.5	.15	1.0	25220.	6226.
6.16	2.00	35.93	.11	2.0	18.5	0.0	1000.	108.	269.	57.6	63.0	188.		25488.	814.	0.0	0.0	.03	1.0	0.	0.
4.26	2.00	29.40	.08	2.0	15.4	3.09	1000.	108.	251.	35.9	63.0	169.		24806.	1068.	7.5	3.1	.16	1.0	25495.	5048.
5.19	2.00	34.96	.05	3.0	18.5	0.0	1000.	108.	243.	36.0	63.0	162.		23689.	1266.	0.0	0.0	.03	1.0	0.	0.
3.75	2.00	28.89	.04	3.0	15.4	3.09	1000.	108.	235.	23.1	63.0	154.		23350.	1628.	7.5	3.1	.16	1.0	25495.	5048.
6.69	2.00	37.10	.11	2.0	18.9	3.79	1250.	110.	285.	62.2	63.0	209.		25899.	777.	9.8	3.8	.17	1.0	25481.	4111.

ALUMINIUM

BASED ON MAX BENDING=70,000 PSI,MAX SHEAR=30,000 PSI, SHEAR AND BENDING STRESSES BELOW IN PSI;T,R IN INCHES

		FUSELAGE SPAR				SAIL DATA			WEIGHT DATA					COMPUTED STRESSES		WINGTIP SPAR				COMPUTED STRESS	
X	Y	LENGTH	T	R	CO	CT	AREA	SPAN	BODY	WFUSE	WSPARS	A/C		BENDING	SHEAR	WEIGHT	LENGTH	T	R	BENDING	SHEAR
1.56	2.00	17.15	.03	2.0	9.1	1.81	500.	92.	211.	7.8	65.0	120.		30290.	2849.	1.4	1.8	.05	1.0	67388.	22731.
2.71	2.00	23.84	.03	2.0	12.8	2.55	750.	98.	215.	10.9	71.0	138.		47124.	2849.	2.1	2.6	.06	1.0	68104.	16314.
5.03	2.00	35.88	.04	2.0	19.2	0.0	1000.	104.	223.	19.2	75.0	156.		68258.	2442.	0.0	0.0	.03	1.0	0.	0.
3.91	2.00	29.94	.03	2.0	16.0	3.21	1000.	104.	219.	13.7	75.0	153.		63757.	2849.	2.9	3.2	.06	1.0	68613.	13082.
5.33	2.00	36.17	.03	3.0	19.2	0.0	1000.	104.	230.	24.8	75.0	163.		36630.	1899.	0.0	0.0	.03	1.0	0.	0.
4.21	2.00	30.25	.03	3.0	16.0	3.21	1000.	104.	228.	20.8	75.0	161.		29628.	1899.	2.9	3.2	.06	1.0	68613.	13082.
5.45	2.00	36.38	.04	2.0	19.3	3.86	1250.	108.	230.	22.2	76.0	171.		62765.	2137.	3.8	3.9	.07	1.0	68425.	10838.
6.90	2.00	42.38	.05	2.0	22.3	4.46	1500.	112.	240.	29.1	74.0	183.		68216.	1899.	4.8	4.5	.07	1.0	68859.	9426.

```
C  PLOT OF WL/B VS B  FROM EQUATING P(CR) WITH P(LOAD)
C  K1=C1  ETC.   ZO=RO/B  ZI=RI/B  KD=DK  KT=TK  EL=L/C   SIGMA=LB/FT**2
C  Y=WL/B   TOP=NUMERATOR   BOTTOM=DENOMINATOR
      DIMENSION Y(200),A(200)
   13 READ(5,100,END=15)DK,H,SIGMA,TK,EL,Q,X,S
      READ(5,100,END=15)WB
      SIGMA=.0193
  100 FORMAT(8F10.5)
      WRITE(6,103)
  103 FORMAT('0',8F10.6)
      SF=1.5
      PIE=3.14159
      ROEM=174.79
      E=1.44E9
      C1=(SIGMA*S)/(1.+TK)
      C2=1.+TK+(WB/(SIGMA*S))
      C3=(1.-1./(6.*EL))/(1.+TK)
      WRITE(6,102)
  102 FORMAT('1',F10.6)
      START=25.
      ZI=1./Q
      ZO=X*ZI
      DO 10 I=1,100
      B=START+FLOAT(I)
      A(I)=B
      AC=(B*H)/(DK*S)
      BP=(256.*(PIE**2)*E*(ZI**2)*H)/(ROEM*(B**2)*SF)
      B1=(256.*(PIE**2)*E*(ZO**2)*H)/(ROEM*(B**2)*SF)
      BRAC=(-AC/2.+2.*(B1+BP)+AC*(1.5*BP+B1))/((1.+B1)*(1.+2.*BP))
      TOP=C1*C2-SIGMA*S*BRAC
      BOTTOM=B*C3-B*BRAC
      Y(I)=TOP/BOTTOM
   10 CONTINUE
      CALL PLOTP(A,Y,100,4)
    7 CONTINUE
      WRITE(6,35)Q,X
   35 FORMAT(20X,'PLOT OF WL/B VS B  Q=',F4.0,2X,'X=',F3.1,2X,'SF=1.5')
      WRITE(6,36)
   36 FORMAT('0',10X,'ASSUMPTIONS')
      WRITE(6,37)
   37 FORMAT(1X,'FT2',4X,'LB/FT2',1X,'LB',2X,'FT')
      WRITE(6,38)
   38 FORMAT(1X,'SAIL',3X,'SIGMA',2X,'WB',2X,'H',3X,'KT',2X,'KD',2X,'L')
      WRITE(6,39)S,SIGMA,WB,H,TK,DK,EL
   39 FORMAT(F6.0,1X,F6.5,1X,F4.0,1X,F2.0,1X,F3.2,1X,F3.2,1X,F3.1)
  111 FORMAT('0',20X,'DATA IS TABULATED USING ALUMINIUM COMPONENTS')
      WRITE(6,111)
      GO TO 13
```

```
      WRITE(6,777)
  777 FORMAT('1')
   15 STOP
      END
//GO.SYSIN DD *
```

.1 211.	4.	.00521	.2	1.5	375.	1.1	500.
.1 216.	4.	.00521	.2	1.5	400.	1.1	750.
.10 220.	4.	.00521	.2	1.5	420.	1.1	1000.
.10 231.	4.	.00521	.2	1.5	450.	1.1	1250.
.1 246.	4.	.00521	.2	1.5	475.	1.1	1500.

```
C  TABULATED VALUES FOR SELECTED WING SPAR CRITERIA
C  OPTIMIZATION UTILIZING SELECTED REFINEMENTS
C  K'=.24+3.25X-4.5X**2=CAYP    X=EX=H/B, WHERE H=HEIGHT ABOVE GROUND(ASSUME=10'
      DIMENSION Y(150)
   13 READ(5,100,END=15)DK,H,SIGMA,TK,WB,EL
  100 FORMAT(8F10.5)
      J=5
      REAL*4 BODY(5)/211.,216.,220.,231.,246./
      REAL*4 D(5)/500.,750.,1000.,1250.,1500./
      REAL*4 X(5)/1.1,1.1,1.1,1.1,1.1/
      REAL*4 Q(5)/375.,400.,420.,450.,475./
      REAL*4 A(5)/90.,97.,103.,104.,106./
      WRITE(6,14)
   14 FORMAT('1',6X,'COMPUTER  VARIATIONS',6X,'WEIGHT   ANALYSIS',10X,
     1'STRUCTURAL  ANALYSIS',12X,'FLIGHT  ANALYSIS  1 MILE FIG.8')
      SF=1.5
      WRITE(6,20)
   20 FORMAT('0',1X,'FT**2',13X,'FT',9X,'TOTAL    FUSE    SPARS',8X,'LBS',
     18X,'INCHES',5X,'INCHES',5X,'HP    FT/S',15X,'SEC',2X,'P(GE)')
      WRITE(6,21)
   21 FORMAT('0',3X,'S',4X,'B/RI   X    SPAN WL/B     WL',4X,'WB    WI   WO
     1   PI',5X,'PO',5X,'RI    RO    TI     TO    P(R)    V',5X,'CL     AR   T
     2.O.F.',3X,'HP')
      WRITE(6,100)
      ETAP=.8
      RCEA=.002377
      PIE=3.14159
      DELX=.01
      DELXB=.3
      DELQB=.05
      DELQ=.5
      SIGMA=.0193
      RCEM=174.8
      E=1.454E+9
      EFF=.75
      FMAN=3.5
      DO 10 I=1,J
      WB=BODY(I)
      S=D(I)
      B=A(I)
    9 CONTINUE
      ZI=1./Q(I)
      ZC=X(I)*ZI
      C1=(SIGMA*S)/(1.+TK)
      C2=1.+TK+(WB/(SIGMA*S))
      C3=(1.-1./(6.*EL))/(1.+TK)
C  Y=WL/B    TOP=NUMERATOR    BOTTOM=DENOMINATOR
      AC=(B*H)/(DK*S)
```

```
      BP=(256.*(PIE**2)*E*(ZI**2)*H)/(ROEM*(B**2)*SF)
      B1=(256.*(PIE**2)*E*(ZO**2)*H)/(ROEM*(B**2)*SF)
      BRAC=(-AC/2.+2.*(B1+BP)+AC*(1.5*BP+B1))/((1.+B1)*(1.+2.*BP))
      TOP=C1*C2-SIGMA*S*BRAC
      BOTTOM=B*C3-B*BRAC
      Y(I)=TOP/BOTTOM
      RO=12.*B*ZO
      RI=12.*B*ZI
      WL=B*Y(I)
      WLP=WL-SIGMA*S
      WO=WLP*(1.+(3./4.)*AC)/(1.+B1)
      PO=((WLP*B**2)/(32.*DK*S))*(3./2.+2./AC)-(WO*B)/(16.*H)
      WI=WLP*((5./4.)*AC+1.*AC*B1-1.+2.*B1)/((1.+B1)*(1.+2.*BP))
      PI=((WLP*B**2)/(32.*DK*S))*(2.+(4./AC))-(3.*WO*B)/(16.*H)-(WI*B)/(
     116.*H)
C   TO AND TI BASED ON EULER BUCKLING EQN
      TI=(PI*((B/4.)**2))/(PIE**3*E*((ZI*B)**3)*2.04)
      TII=SF*TI
      IF(TII-.0025)1,2,3
    3 DELQ=-1.*ABS(DELQ)
      DELQB=-1.*ABS(DELQB)
      GO TO 11
    1 DELQ=ABS(DELQ)
      DELQB=ABS(DELQB)
   11 IF((ABS(TII-.0025))-.0000833)2,2,4
    4 TII=TII+DELQ
      B=B+DELQB
      Q(I)=Q(I)+DELQ
      L=L+1
      GO TO 9
    2 CONTINUE
      TO=(PO*((B/4.)**2))/(PIE**3*E*((ZO*B)**3))
      TOO=SF*TO
      IF(TOO-.0025)7,6,5
    5 DELX=ABS(DELX)
      DELXB=ABS(DELXB)
      GO TO 25
    7 DELX=-1.*ABS(DELX)
      DELXB=-1.*ABS(DELXB)
   25 IF((ABS(TOO-.0025))-.0000833)6,6,8
    8 TOO=TOO+DELX
      B=B+DELXB
      X(I)=X(I)+DELX
      M=M+1
      GO TO 9
    6 CONTINUE
      TII=12.*TII
      TOO=12.*TOO
```

```
      F=FMAN+.25*(2.*ZI+2.*ZO)*((A(I)**2)/2.)
      P=(4.*(SQRT(2./ROEA))*(Y(I)**1.5)*(F**.25))/
     1(550.*ETAP*(3.*EFF*PIE)**.75)
      V=(SQRT((2.*Y(I))/ROEA))/((3.*PIE*EFF*F)**.25)
      CUE=(ROEA/2.)*(V**2)
      CL=WL/(CUE*S)
      AR=(B**2)/S
      EX=.1
      CAYP=.24+3.25*EX-4.5*(EX**2)
      CDI=(CAYP*(CL**2))/(PIE*AR)
      PGE=(CUE*V/550.)*(F+(CDI*S)/EFF)*ETAP
C 1 MILE COURSE W/300 FT TURN RADIUS +10%
      TOF=(1.1*(5280.+2.*PIE*300.))/V
      WRITE(6,30)S,Q(I),X(I),B,Y(I),WL,WB,WI,WO,PI,PO,RI,RO,TII,TOO,
     1P,V,CL,AR,TOF,PGE
   30 FORMAT(F6.0,2X,F4.0,1X,F4.2,1X,F4.0,1X,F5.3,2X,F5.1,2X,F4.0,2X,
     1F3.0,1X,F3.0,2X,F6.0,1X,F6.0,2X,F3.1,1X,F4.1,1X,F5.4,1X,F5.4,2X,
     2F4.2,2X,F4.1,2X,F4.2,2X,F4.1,2X,F5.1,3X,F5.3)
   10 CONTINUE
      WRITE(6,111)
  111 FORMAT('0',20X,'DATA IS TABULATED USING ALUMINIUM COMPONENTS,SF=1.
     15,     TAPERED WING WITH CT/CO=.2,EFF=.75  2.2 OZ SAIL')
      WRITE(6,112)
  112 FORMAT(20X,'GROUND EFFECT COMPUTATIONS USING ALTITUDE=10% OF B')
      WRITE(6,36)
   36 FORMAT('0',10X,'ASSUMPTIONS')
      WRITE(6,38)
   38 FORMAT(          8X,'SIGMA',2X,'WB',2X,'H',3X,'KT',2X,'KD',2X,'L')
      WRITE(6,37)
   37 FORMAT(          8X,'LB/FT2',1X,'LB',2X,'FT')
      WRITE(6,39)  SIGMA,WB,H,TK,DK,EL
   39 FORMAT(     7X,F6.5,1X,F4.0,1X,F2.0,1X,F3.2,1X,F3.2,1X,F3.1)
      WRITE(6,777)
  777 FORMAT('1')
   15 STOP
      END
//GO.SYSIN DD *
  .1      4.        .00521     .2        240.     1.5
```

S/K


BLA

```
C   FUSELAGE SPAR SHEAR,MOMENT,WEIGHT,BALANCE ANALYSIS
C   WINGTIP SPAR SHEAR,MOMENT,WEIGHT ANALYSIS
C   READ IN ALL VALUES IN LBS,FT, OR COMBINATIONS THEREOF
C   X=DIST OF MAN/BIKE FROM CG, Y=DIST PROP IS IN FRONT OF MAN
C   V=R2*SIN(TAN-1(4/B/4))=158@SPAR VS 190 @MAN
    20 FORMAT('1',F10.8)
       WRITE(6,20)
       WRITE(6,23)
    23 FORMAT('0',10X,'BASED ON MAX BENDING=70,000 PSI,MAX SHEAR=30,000
      1PSI, SHEAR AND BENDING STRESSES BELOW IN PSI;T,R IN INCHES')
       WRITE(6,50)
    50 FORMAT('0',13X,'FUSELAGE SPAR       SAIL DATA        WEIGHT DATA',
      113X,'COMPUTED STRESSES  WINGTIP SPAR          COMPUTED STPESS')
       WRITE(6,51)
    51 FORMAT('0','   X     Y   LENGTH  T    R    CO    CT  AREA  SPAN BODY WF
      1USE  WSPARS  A/C    BENDING    SHEAR  WEIGHT LENGTH  T    R  BENDING
      2 SHEAR')
       WRITE(6,778)
   778 FORMAT('0')
    25 READ(5,100,END=15)WPROP,WMAN,WBIKE,WSPARS,SIGMAS
       READ(5,100,END=15)TF,RF,TRATIO,S,B,WL,RS,TS
   100 FORMAT(8F10.5)
       DK=.1
       EPS=0.00041667
       V=358.
C   V=190+10+158
       SIGMAS=.0193
       SF=1.5
       TAUMX=4.32E+6
       SIGMX=1.008E+7
       WSAIL=S*SIGMAS
       ROEM=174.79
       PIE=3.14159
C   TIP SPAR BENDING
       CO=(2.*S)/(B*(1.+TRATIO))
       CT=CO*TRATIO
       IF(TRATIO)28,40,28
    28 CONTINUE
       WLP=WL-SIGMAS*S
       CONST=(WLP*B**2)/(32.*DK*S)
       TLEJ=CONST*(3./8.)
       TJ=2.*TLEJ
       TM=CONST/4.
       EMS=TLEJ*(CT/2.)
    29 BENDSP=(EMS*SF)/(PIE*TS*RS**2)
       IF(SIGMX-BENDSP)30,31,31
    30 TS=TS+EPS
       GO TO 29
```

```
   31 CONTINUE
C  TIP SPAR SHEAR
      VS=TLEJ+TJ+TM
      SHEARS=(VS*SF)/(PIE*RS*TS)
      IF(TAUMX-SHEARS)32,33,33
   32 TS=TS+EPS
      GO TO 29
   33 GO TO 41
   40 WTIPSP=0.
      SHEARS=0.
      BENDSP=0.
      GO TO 99
   41 WTIPSP=2.*(2.*PIE*RS*TS*CT*ROEM)
C  BALANCE COMPUTATION
   99 Y=2.0
      C1=ROEM*PIE*RF*TF
      WTAIL=.2*(WSPARS+WSAIL)
      C2=WPROP
      C3=WMAN+WBIKE
      C4=(WSPARS+WSAIL)*(CO/6.)+WTAIL*(1.5*CO-1.5)+C1*((1.5*CO)**2)
    1 G=2.*Y+C2/C1+C3/C1
      C=Y**2+(C2/C1)*Y-C4/C1
      ROOT=SQRT(G**2-4.*C)
      X=(ROOT-G)/2.
      IF((X+Y)-(CO/3.))3,3,5
    3 Y=Y+.1
      GO TO 1
    5 CONTINUE
      EL=X+Y+1.5*CO
C  WEIGHT COMPUTATION
      WFUSE=ROEM*2.*PIE*RF*TF*EL
      WBODY=WFUSE+WMAN+WPROP+WBIKE+.2*WFUSE+WTIPSP
      WAC=WBODY+1.2*(WSPARS+WSAIL)-180.
C  MOMENT ANALYSIS  REFER PILKEY P.271
      EM1=WPROP*(X+Y+CO/6.)
      EM2=(WBIKE+WMAN)*(X+CO/6.)
      EMT=EM1+EM2
      VALUE=(EMT*SF)/(PIE*RF**2*TF)
      IF(SIGMX-VALUE)2,4,4
    2 TF=TF+EPS
      GO TO 99
    4 CONTINUE
C  SHEAR ANALYSIS REFER PILKEY P.272
      TAU=(V*SF)/(PIE*RF*TF)
      IF(TAUMX-TAU)6,7,7
    6 TF=TF+EPS
      GO TO 99
    7 CONTINUE
```

```
      TAU=TAU/144.
      BENDSP=BENDSP/144.
      SHEARS=SHEARS/144.
      VALUE=VALUE/144.
      RF=12.*RF
      TF=12.*TF
      RS=12.*RS
      TS=12.*TS
      WRITE(6,52)X,Y,EL,TF,RF,CO,CT,S,B,WBODY,WFUSE,WSPARS,WAC,VALUE
     1,TAU,WTIPSP,CT,TS,RS,BENDSP,SHEARS
   52 FORMAT(    F5.2,1X,F4.2,2X,F5.2,1X,F3.2,1X,F3.1,1X,F4.1,1X,F4.2,1X
     1F5.0,1X,F4.0,1X,F4.0,2X,F4.1,2X,F4.1,3X,F4.0,3X,F7.0,2X,F7.0,
     22X,F4.1,3X,F4.1,1X,F3.2,1X,F3.1,2X,F7.0,1X,F7.0)
      GO TO 25
   15 STOP
      END
//GO.SYSIN DD *
  10.       180.      10.       65.       .00521
 .0025      .16667    0.2       500.       90.      336.5     .08333    .0025
  10.       180.      10.       68.       .00521
 .0025      .16667    0.2       750.      97.       352.3     .08333    .0025
  10.       180.      10.       74.       .00521
 .0025      .16667    0.2       1000.     103.      370.8     .08333    .0025
  10.       180.      10.       78.       .00521
 .0025      .16667    0.2       1250.     104.      395.0     .08333    .0025
  10.       180.      10.       87.       .00521
 .0025      .16667    0.2       1500.     106.      430.6     .08333    .0025
```

LIST OF REFERENCES

1. Gerald,C.F., Applied Numerical Analysis, p. 34 to 39, Addison-Wesley, 1970.

2. Gerard,G. and Steinbacker,F.R., Aircraft Structural Mechanics, p. 225, Pitman Publishing Corp.,N.Y., 1952.

3. Glauert H., The Elements of Aerofoil and Airscrew Theory, p. 152, Cambridge, 1959.

4. Hurt,H.,H., Aerodynamics for Naval Aviators, p. 380, NAVWEPS 00-80T-00, revised 1965.

5. Metals Haddbook,eighth ed.,v.1, American Society for Metals, p. 948, Metals Park, Ohio, 1961.

6. Parker,J.F. and West,V.R., Bioastronautics Data Book,(NASA SP-3006), p. 867, Scientific and Technical Information Office, 1973.

7. Pilkey,O.H. and Pilkey,W.D., Mechanics of Solids, p. 151,216,269,278,389, Quantum Publishers, 1974.

8. Sherwin,K., Man Powered Flight, p. whole text, Argus Press Ltd.,London, 1971.

9. Strong,C.L., "Amateur Scientist", p. Scientific American v.231, 138 to 143, Dec 74.

10. Von Mises,R., Theory of Flight, p. 100,106, Dover Publications Inc., 1959.

INITIAL DISTRIBUTION LIST

		No. Copies
1.	Defense Documentation Center Cameron Station Alexandria, Virginia 22314	2
2.	Library,Code 0212 Naval Postgraduate School Monterey, California 93940	2
3.	Department Chairman, Code 67 De partment of Aeronautics Naval Postgraduate School Monterey, California 93940	1
4.	Provost Emeritus M. U. Clauser Naval Postgraduate School Monterey California 93940	1
5.	Doctor K. Sherwin Department of Mechanical Engineering University of Liverpool Liverpool, England	1
6.	Lt Lynn Carter II, USN Fitron 101 NAS Oceana, Virginia	1